1978-12

Investigation of electrode materials for low frequency electric antennas in sea water

Dearth, Lawrence Charles

Monterey, California. Naval Postgraduate School

NAVAL POSTGRADUATE SCHOOL
Monterey, California

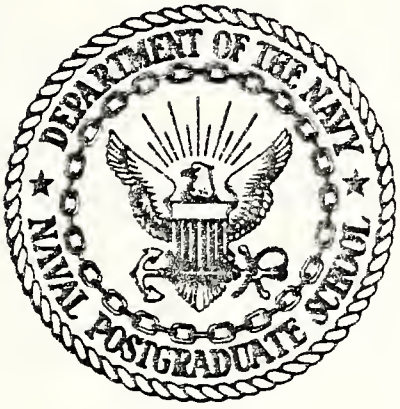

THESIS

INVESTIGATION OF ELECTRODE MATERIALS
FOR LOW FREQUENCY ELECTRIC ANTENNAS
IN SEA WATER

by

Lawrence Charles Dearth

December 1978

Thesis Advisor: Paul H. Moose

Approved for public release; distribution unlimited.

REPORT DOCUMENTATION PAGE

READ INSTRUCTIONS BEFORE COMPLETING FORM

1. REPORT NUMBER

2. GOVT ACCESSION NO.

3. RECIPIENT'S CATALOG NUMBER

4. TITLE (and Subtitle)
Investigation of Electrode Materials for Low Frequency Electric Antennas in Sea Water

5. TYPE OF REPORT & PERIOD COVERED
Master's Thesis; December 1978

6. PERFORMING ORG. REPORT NUMBER

7. AUTHOR(s)
Lawrence Charles Dearth

8. CONTRACT OR GRANT NUMBER(s)

9. PERFORMING ORGANIZATION NAME AND ADDRESS
Naval Postgraduate School
Monterey, California 93940

10. PROGRAM ELEMENT, PROJECT, TASK AREA & WORK UNIT NUMBERS

11. CONTROLLING OFFICE NAME AND ADDRESS
Naval Postgraduate School
Monterey, California 93940

12. REPORT DATE
December 1978

13. NUMBER OF PAGES

14. MONITORING AGENCY NAME & ADDRESS(if different from Controlling Office)

15. SECURITY CLASS. (of this report)
Unclassified

15a. DECLASSIFICATION/DOWNGRADING SCHEDULE

16. DISTRIBUTION STATEMENT (of this Report)
Approved for public release; distribution unlimited.

17. DISTRIBUTION STATEMENT (of the abstract entered in Block 20, if different from Report)

18. SUPPLEMENTARY NOTES

19. KEY WORDS (Continue on reverse side if necessary and identify by block number)

20. ABSTRACT (Continue on reverse side if necessary and identify by block number)

This paper describes and gives the results of an experiment to measure the D.C. and ULF (0.1 to 1 Hz) relative impedance in sea water of several materials considered as possible electrodes for a submerged electric dipole antenna. The results of the ac and dc impedance tests are given for Ag, Al, C, Cu, Ni, Pb, Pt, Sn, Ti, W, Zn, and Stainless Steel, in the form of potential differences vs current and impedance vs frequency curves. Tests concerning the relative receiving impedance of Silver Silver-Chloride, Platinum Platinum-Black,

carbon,and zinc electrodes are reported. A comparison is made between the submerged magnetic loop and electric dipole antennas for characteristics of open circuit voltage, short circuit current, antenna gain, and noise, Based on the analytical and experimental results obtained recommendations are made to further test the impedance and noise characteristics of the Silver Silver-Chloride, Platinum Platinum-Black, and carbon electrodes.

INVESTIGATION OF ELECTRODE MATERIALS FOR LOW FREQUENCY ELECTRIC ANTENNAS IN SEA WATER

by

Lawrence Charles Dearth
Lieutenant Commander, United States Navy
B.S., University of Idaho, 1966

Submitted in partial fulfillment of the
requirements for the degree of

MASTER OF SCIENCE IN PHYSICS

from the

NAVAL POSTGRADUATE SCHOOL
December 1978

ABSTRACT

This paper describes and gives the results of an experiment to measure the D.C. and ULF (0.1 to 1 Hz) relative impedance in sea water of several materials considered as possible electrodes for a submerged electric dipole antenna. The results of the ac and dc impedance tests are given for Ag, Al, C, Cu, Ni, Pb, Pt, Sn, Ti, W, Zn, and Stainless Steel, in the form of potential difference vs current and impedance vs frequency curves. Tests concerning the relative receiving impedance of Silver Silver-Chloride, Platinum Platinum-Black, carbon and zinc electrodes are reported. A comparison is made between the submerged magnetic loop and electric dipole antennas for characteristics of open circuit voltage, short circuit current, antenna gain, and noise. Based on the analytical and experimental results obtained recommendations are made to further test the impedance and noise characteristics of the Silver Silver-Chloride, Platinum Platinum-Black, and carbon electrodes.

TABLE OF CONTENTS

LIST OF FIGURES

I. INTRODUCTION

Fluctuations of the geomagnetic field with periods of a day or less have been known to exist for well over two centuries [Graham 1724]. But only in the last few decades, as ever more sensitive magnetometers were developed in response to military and geophysical exploration requirements, have systematic investigations of these complex fluctuations become possible. For land based observations, it is now generally agreed that most of the field variations are generated by current systems flowing in the ionosphere and magnetosphere and by the response of the geomagnetic field to fluctuations in the solar wind. Sea based observations are complicated by the presence of a moderately good conductor (sea water) and complex propagation phenomena associated with the geology of the ocean floor. The study of ambient magnetic fields in the ocean has traditionally been concentrated in two areas (i) magnetic anomalies due to geological features of the ocean floor [Vacquier 1972] and (ii) variations in the ambient field produced by magnetic objects (usually man made) at or near the ocean surface. In particular, the magnetic anomaly introduced into the earth's field by steel hulled ships has been used successfully for mine, torpedo, and antisubmarine warfare over the last forty years.

Another application in which the low frequency electromagnetic background noise is important is in the field of undersea communications. Since the skin depth increases at low frequency, ULF (ultra low frequency, $\leq$ 5 Hz) waves can penetrate the ocean to great depths and may be used to communicate with submarines [Fraser-Smith et al, 1977]. Reliable

reception of signals of limited power requires high receiver sensitivity and low ambient background noise at the depth of the receiver [Dinger et al, 1977]. Since the advent of the superconducting magnetometer, the potential threshold of signal detection is well below the level of random fluctuations or noise which is observed in the ambient magnetic field near the earth's surface [Fraser-Smith and Buxton 1975, Gillespie et al, 1977].

Another source of noise which limits signal detectability is equipment or system noise [Skolnik 1962]. This is noise which is generated in the detection equipment itself, or at the interface of the equipment and the medium in which the signal is being detected. If system noise can be identified, steps can normally be taken to eliminate it completely or at least reduce it to acceptable limits. Background noise on the other hand, cannot be eliminated. However, if it can be identified, and correlated, it's effects can be greatly reduced by using modern techniques of signal processing [Etro 1978].

Although measurements on the ocean floor using superconducting magnetometers have been carried out, the logistic and engineering problems, such as cryogenic atmosphere are considerable [Dinger et al, 1977]. Because of the engineering difficulties incurred with the superconducting magnetometers, other means of signal detection are being examined. These include optically pumped magnetometers [Barry 1978], magnetic loop antennas [Bannister 1977, Dunckel 1969], and electric dipole antennas [Strarup 1966, Wait 1952]. While the sensitivity of these systems admittedly does not approach that of the superconducting magnetometer, it is generally agreed that they can be used effectively to gain the information on the background noise which is currently not fully understood.

During the spring of 1977, undersea measurements of electromagnetic signals were begun by Naval Postgraduate School (NPS), in conjunction with the Stanford Electronics Research Laboratory. The early measurements were made to determine the feasibility of using a self-contained system resting on the ocean floor to measure background noise. A block diagram of the system designed by the Stanford group is shown in Fig. 1. This system, designed to operate between 100 Hz and 1 kHz, consisted of a fifty-seven turn circular open core loop with a diameter of 106 cm, two single stage, common source configured zn4869aj FET amplifiers and a Panasonic model RQ-3235 portable cassette tape recorder and was mounted in a pressure vessel by NPS personnel as shown in Fig. 2.

Throughout the summer of 1978, the system was tested from the NPS research vessel ACANIA, in 250 feet of water approximately three miles west of Moss Landing, in Monterey Bay. Several system noise sources were systematically identified and eliminated or reduced.

By the spring of 1978, the equivalent noise level of the system had been reduced to the order of 10^{-9} $(nT^2)/Hz$, at 100 Hz. Further improvements in the antenna design, frequency range, signal amplification and recording, and stability are currently being made.

Figures 3 and 4 show the configuration of the amplifier and recorder in the pressure vessel and Fig. 5 shows the system ready for deployment on the fantail of R/V ACANIA.

During the spring of 1978, investigations into the feasibility of using an electric dipole antenna for below surface measurements was begun by NPS. The following sections of this paper report on these studies and the progress made to date.

II. THEORY

A. ANTENNAS IN A CONDUCTING MEDIUM

Background noise investigations on land have long relied on electric dipole antennas. The behavior and characteristics of these antennas above ground is well documented [Shadowitz 1975]. The behavior of antennas immersed in a conducting medium is however, quite different than that of the corresponding antenna in air [Moore 1963]. The normal methods of determining radiation resistance, antenna gain and antenna patterns are no longer valid when the antenna is in a conducting medium. As an example, the standard technique for computing the radiation resistance of an antenna in air is to compute the average flow of power across a sphere surrounding the antenna. The resistance may then be determined by dividing this power by one half the square of the peak value of the input current. In air the size of the sphere is not important because the same average power flows through a sphere of essentially any radius. In the conducting medium, however, the size of the sphere makes a great deal of difference. Power dissipation, especially in the immediate vicinity of the antenna, causes the average power flowing across different size spheres to vary widely.

B. ELECTROMAGNETIC PROPAGATION IN SEA WATER

In the ocean the principal features of electromagnetic wave propagation are well understood. Kraichman has published handbooks for conducting media that give many of the relevant formulas in considerable detail [Kraichman 1976]. Sea water with a conductivity of about four Siemens/m, lies roughly halfway between good insulators (5×10^{-9} Siemens/m) and good conductors ($5 \times 10^{+7}$ Siemens/m).

The effect of the sea water's relatively high conductivity is to a) reduce the freespace wavelength and phase velocity by several orders of magnitude, b) introduce dispersion, since the propagation constant is a non-linear function of frequency, and c) induce losses, as described by the complex propagation constant. Attenuation of a signal in sea water with a conductivity of four Siemens/m is equal to 55db/wavelength, independent of frequency. At 1 Hz, a wavelength is about 1.6 kilometer, at .01 Hz a wavelength is about 16 kilometers and at 100 Hz a wavelength is 160 meters.

If a plane wave is incident on the ocean surface, most of the energy is reflected, but a small portion is transmitted into the ocean. The large phase velocity contrast ($v_{\text{sea water}}/v_{\text{air}} < 10^{-4}$) between sea water and the atmosphere causes the transmitted wave to be refracted straight down, essentially independent of the angle of incidence of the incoming wave[1]. Since the field components of a plane wave are perpendicular to the propagation direction, all field components of the transmitted wave are horizontal.

Wave vector diagrams are shown in Fig. 6(a) and 6(b), for transverse magnetic and transverse electric waves respectively. In Fig. 6 the subscripts o, r, and t stand respectively for incident, reflected, and transmitted. In Fig. 6(a), H_o, H_r, and H_t, are all out of the paper and the field relationships are as follows:

$$H_o = \frac{E_o}{\eta_o} \quad , \quad H_r = \frac{E_r}{\eta_o}$$

$$H_t = H_o + H_r \simeq 2H_o$$

[1] Ninety degree angle of incidence must be treated by special methods [Kraichman 1976].

$$E_t = \eta_{sw} H_t = 2 \frac{\eta_{sw}}{\eta_o} E_o$$

Where η_o and η_{sw} are the intrinsic impedances of air and sea water respectively. For the transverse electric wave in Fig. 6(b), E_o and E_t are into paper while E_r is out of the paper. The field relationships for the transverse electric case are given by the following:

$$H_o = \frac{E_o}{\eta_o} \quad , \quad H_r = \frac{E_r}{\eta_o}$$

$$H_T = H_o \cos \theta_o + H_r \cos \theta_o \sim 2 H_o \cos \theta_o$$

$$E_T = \eta_{sw} H_T = 2 \cos \theta_o \left(\frac{\eta_{sw}}{\eta_o}\right) E_o$$

From the above relationships it can be seen that the transmitted magnetic field just below the surface is approximately twice the transverse component of the incident magnetic field. The transmitted electric field however, is reduced by the relative impedance of sea water in the T.M. case and by the relative impedance times the cosine of the angle of incidence in the T.E. case. The absolute value of the relative impedance of sea water with conductivity of 4 Siemen/m, varies from 10^{-7} for a frequency of .001 Hz to 2.5×10^{-5} for a frequency of 100 Hz. Hence, the transmitted E field is from four to seven orders of magnitude less than the incident field. Further attenuation with depth at 55 db/wavelength will require an extremely sensitive, low noise antenna for E field detection.

C. THE ELECTRIC DIPOLE ANTENNA

1. Dipole Impedance

The electric dipole antenna consists of a simple electrode pair

that senses the potential difference between two points in the medium. Since the electrodes detect the tangential component of electric field, only horizontal electrodes are discussed in this report.

Fig. 7 is a diagram of a simple dipole antenna. Electrodes are located at points A and B and l is the distance between the electrodes. In the presence of a horizontal electric field, E, with a tangential component along the axis of the dipole, the difference in potential between the electrodes is given as:

$$V_{AB} = \int_A^B \vec{E} \cdot d\ell$$

and in the special case where the dipole axis is parallel to E,

$$V_{AB} = E\ell$$

An equivalent electrical circuit is shown in Fig. 8 where Z_o is the dipole impedance and Z_w is the sea water impedance. The total impedance is given by:

$$Z_t = \frac{Z_D Z_w}{Z_D + Z_w}$$

Since Z_D is typically less than 0.5 ohm and for sea water with σ = 4 S/M, and a dipole length of 100 m, Z_w is on the order of 20Ω, $Z_D << Z_w$ and in general

$$Z_t \approx Z_D$$

The current through the dipole antenna is then given by:

$$I_D = \frac{E\ell}{Z_D}$$

The dipole impedance is composed of several terms and can be represented by the electrical circuit in Fig. 9, from which:

$$Z_D = 2\,R_e + \left[\frac{(R_w + R_r + j\omega L_w)\,\frac{1}{j\omega C_w}}{R_w + R_r + j\omega L_w + \frac{1}{j\omega C_w}} \right]$$

where:

R_e = electrode resistance

R_w = Ohmic resistance of the wire

R_r = Radiation resistance of the wire

L_w = Inductance of the wire

C_w = Capacitance between wire and water

The radiation impedances for an infinite one wire cable have been computed [Oldenbury 1920], and are found to be:

$$R_r = 10^{-1}\,\pi\,f\ \Omega/m$$

$$L_w = [12.6 - \ell n(b^2\sigma f)]\,10^{-7}\ H/m$$

$$C_w = \frac{2\pi E}{\ell n\,\frac{c}{b}}\ F/m$$

$$R_w = \frac{1}{\sigma_w a}\ \Omega/m$$

where:

a is the cross section of the wire

σ_w is the conductivity of the wire

σ is the conductivity of the water

E is the dielectric constant of the wire insulator

b & c are the inner and outer radii respectively of the wire insulating material

From this the wire impedance is seen to be:

$$Z_w = \left[\frac{(R_w + R_r + j\omega L_w)\,\frac{1}{j\omega C_w}}{R_w + R_r + j\omega L_w + \frac{1}{j\omega C_w}} \right]$$

For low frequencies and normal copper wire values,

$$\frac{1}{j\omega C_w} >> j\omega L_w + R_w + R_r$$

hence, the equation for Z_w reduces to

$$Z_w = R_w + R_r + j\omega L_w$$

and the total dipole impedance reduces to

$$Z_D = 2\,R_E + R_w + R_r + j\omega L_w$$

The impedance of the electrode is taken to be pure resistive [Strarup 1966] and can be computed in the following manner. Consider a spherical electrode, with radius a, as in Fig. 10, located in a conducting medium with conductivity σ. The electrode may then be viewed as a current source surrounded by a radial current density field given by:

$$J = \frac{I}{4\,\pi\,r^2}$$

The electric field strength is:

$$E = \frac{J}{\sigma}$$

The potential on the surface of the sphere is then given by:

$$V = \int_a^\infty \vec{E} \cdot d\vec{N}$$

Substituting for E yields:

$$V = \int_a^\infty \frac{I}{4 \pi \sigma r^2} \, dr = \frac{I}{4 \pi \sigma a}$$

from whence the electrode resistance is found to be:

$$R_E = \frac{V}{I} = \frac{1}{4 \pi \sigma a}$$

when the electrode is a sphere. The electrode resistance varies with the shape of the electrode and had been found in general to be [Strarup 1966]:

$$R_E = \frac{K}{\sqrt{S}}$$

where K is a constant depending on the shape of the electrode and S is the contour surface area. The value of K does not change appreciably from shape to shape, unless one dimension is much larger than the others. For example:

K sphere = 0.14 ohm.m

K disc = 0.16 ohm.m

K prolate Ellip = 0.12 ohm.m for eccentricity 10

K prolate Ellip = 0.08 ohm.m. for eccentricity 50

The total impedance of the dipole is then:

$$Z_D = \frac{2K}{\sqrt{S}} + R_W + 10^{-7} \pi f \ell + j\omega [12.6 - \ell n \, b^2 \sigma f] \ell + 10^{-7}$$

Comparing terms it is seen that at low frequencies and with copper wires with good conductance,

$$2 R_E \simeq \frac{2K}{\sqrt{S}}$$

dominates and hence, Z_D is essentially resistive and equal to the resistance of the electrodes. The experiments described in chapter three of this report indicate that at low frequency there is an additional term in the electrode impedance which is reactive and is ascribed to a polarization effect at the surface of the electrode [Nannestad 1965].

2. Polarization

Electrode polarization can be explained by referring to Fig. 11 where A and B are electrodes in a conducting medium in which there is an electric field $\vec{E}$ as indicated. The dipole acts as a shunt across the field in the medium and electrons will flow into the dipole at A and exit at B. In addition to the electrons, negative ions will be attracted to A and positive ions will be attracted to B. Given sufficient time, these ions form a cloud at the respective electrodes, thereby impeding the current flow through the dipole. As the frequency is increased, these clouds do not have time to form and therefore the impedance is smaller.

3. Antenna Gain

Antenna gain is normally defined as [Skolnik 1962].

$$G = \frac{K^2}{\pi} A_e$$

where K is the free space propagation constant and A_e is the effective area. The effective area of the dipole in a conducting medium has been

shown to be [Hansen 1963]:

$$A_e = 4\ K\ \ell\ \delta^2$$

where ℓ is the antenna length and δ is the skin depth. Combining the above gives:

$$G = \frac{4\ K^3\ \ell\ \delta^2}{\pi}$$

Since $K = \frac{2\pi}{\lambda}$ and ℓ and δ are normally less than λ it can be seen that the gain is less than 1, and determined by ℓ for any given frequency.

4. Antenna Noise

The inherent noise of the dipole antenna in a conducting medium can be broken down into four basic sources:

a. Noise due to motion of the antenna in the earth's static magnetic field

b. Thermal or Johnson noise

c. Water motion noise

d. Electrolysis or corrosion current noise

Each of these sources will be looked at individually. The noise due to motion in the dipole antenna is caused only by lateral motion in the earth's magnetic field. If the strength of the earth's magnetic field at the antenna is B at an inclination of ϕ, then the noise voltage induced in the antenna for a periodic motion of amplitude S_o and frequency ω is given by:

$$V_{NM} = \ell\ \frac{ds}{dt}\ B \sin \phi$$

or

$$V_{NM} = \ell\ \omega\ S_o\ B \sin\phi \cos\omega t$$

where

$$S = S_o \sin\omega t$$

If the antenna is supported from a floating object, stability could be a major problem, however, in a bottom mounted system antenna motion could be largely removed.

Johnson or thermal noise refers to noise voltage due to random motion of charged particles in a conducting medium [Carlson 1975]. This voltage is random and consistent with the central limit theorem, has gaussian distribution with $\bar{v} = o$ and $\bar{v}^2 = \sigma^2 = \frac{2\ (\pi\ k_B\ T)^2}{3h}\ R\ \text{volts}^2$ where k_B is Boltzmans constant, T is the temperature in degrees, Kelvin and h is Planck's constant. This is a form of the Nyquist Theorem [Fenwick and Weeks 1963] with Planck's constant added as a result of quantum mechanical considerations. It is further shown by quantum theory that the spectral density of the noise voltage is given by:

$$G_v(f) = \frac{2\ R\ h\Delta f}{\text{exp.}\ (h\Delta f/k_B T) - 1}\ V^2/Hz$$

For

$$\Delta f = 100 \text{ and } T = T_o = 290°K$$

$$\frac{h\Delta f}{k_B T} = 1.7 \times 10^{-11} << 1$$

Hence

$$\exp\ (h\Delta f/k_B T) \simeq 1 + \frac{h\Delta f}{k_B T}$$

And

$$G_v(f) = \frac{2\ R\ h\Delta f}{1 + \frac{h\Delta f}{k_B t} - 1} = 2\ R\ k_B T \quad V^2/H_z$$

For narrow bands the spectral density is essentially constant and the spectral density of the noise power delivered to load resistance R^1 can be determined from

$$P = \langle I^2 \rangle\ R = \frac{\langle V^2 \rangle\ R^1}{(R + R^1)^2}$$

From basic antenna theory, maximum power transfer is effected when $R = R^1$, therefore:

$$P_{max} = \frac{\langle V^2 \rangle\ R}{4R^2} = \frac{\langle V^2 \rangle}{4R}$$

and in terms of spectral density

$$G_P max = \frac{G_v(f)}{4R} = \frac{2\ R\ k_B T}{4R} = \frac{1}{2}\ k_B T \quad \text{Watts/Hz}$$

From which it is seen that the maximum thermal noise power delivered to the load is independent of the resistance of the antenna.

Noise associated with water motion across the surface of electrodes has been noted previously [Nannestad 1965 and Strarup 1966]. The exact mechanism of the noise is not clearly understood. However, it is theorized that this noise is associated with the polarization. It is

possible that water motion across the surface of the electrode disturbs the ion cloud and noise results from the attempts of the system to regenerate the cloud.

The water motion noise appears to depend on the type of material used for the electrode and the amount of water crossing the exposed surface of the electrode. Methods of reducing this noise which have been successful are wrapping the electrodes in gauze, and enclosing the electrodes in a baffle system. Some caution must be exercised when using these methods however as they both have a tendency to increase the resistance of the electrodes.

Water motion noise was at first believed to be caused by corrosion currents, however after careful studies [Nannestad 1965] covering a period of two years, there was no detected noise which could be correlated with or attributed to corrosion currents.

Of the four noise types discussed, it is worthy to note that only the first, antenna motion noise, depends on antenna length. This becomes extremely important when considering the signal-to-noise ratio. Since most of the antenna noise is independent of antenna length and antenna motion noise can be effectively eliminated by bottom mounting, the signal-to-noise ratio becomes directly proportional to the length of the antenna.

Appendix A contains a quantitative comparison of loop and dipole antennas with respect to the characteristics discussed in this section. The results of the computations show that for a frequency of 1 Hz and a dipole of 100 meters, an equivalent loop antenna (one which develops the same open circuit voltage) has less short circuit current, less gain and higher potential for noise due to motion. Furthermore, the

loop, a point sensor, will not improve its signal-to-noise ratio with respect to water motion noise with increases in sensitivity.

III. EXPERIMENTS

A. PURPOSE

The research of [Strarup 1966, and Nannestad 1965], indicated that the electrode impedance was not linear, especially at low frequency up to 10 Hz. It was also shown that the electrode impedance varied widely depending on the material from which they were constructed. Table 1 is a summary of their findings with respect to electrode impedance in sea water for the materials which they tested. The impedances (resistances) in the table are not absolute, but since conditions were held constant for the various materials they provide a satisfactory relative picture.

In order to verify the results shown in table 1, and to gain additional information on the behavior of electrodes in sea water, experiments were conducted on electrodes made from the materials listed in table 2. Also included in table 2 are several physical constants of the materials which were compared with the data obtained in the experiments. The materials in table 2 are listed in order of their appearance in the galvanic series, (Electromotive potential in sea water), from positive to negative. Tests were conducted on the materials to determine their relative dc resistance, low frequency ac impedance and low frequency receiving impedance.

B. EQUIPMENT

All tests were conducted with the electrodes in a trough measuring 200 x 25 x 25 cm. The trough was lined with plastic and filled with sea water from Monterey Bay. The temperature of the water for the

Material	Z_p OHMS			
	1 Hz	10 Hz	100 Hz	1000 Hz
Stainless Steel	200	60	25	19
Monel	210	40	19	12
Aluminum	720	200	115	35
Aluminum Alloy	700	240	100	30
Bronze	160	50	15	12
Zinc	18	14	13	11
Carbon	450	70	15	10

Table 1 Z vs f (Nannestad, 1965)

Material	$\sigma(\mu\Omega m)^{-1}$	Contact Work Function (ev)	Electro Negativity (v)	Electro Chem Potential (v)
Platinum	.095	4.52	2.2	1.2
Silver	.616	4.35	1.9	.7996
Titanium	.024	4.14	1.5	-2.0
Stainless	-	-	-	-
Nickel	.145	4.75	1.8	- .23
Copper	.593	-	1.9	.522
Tungsten	.181	4.38	1.7	- .04
Tin	.088	4.35	1.8	- .1364
Lead	.046	3.94	1.8	- .1263
Aluminum	.382	3.75	1.5	-1.706
Zinc	.167	4.0	1.6	- .7628
Carbon	.0007	-	2.5	.6992

Table 2 Test Materials

tests was 18° Centigrade. The water was changed prior to each separate experiment in an attempt to maintain constant conductivity.

Electrodes were constructed from the materials in table 2 as shown in Fig. 12. While cylindrical electrodes would have been more desirable, most of the available material was in sheets, so flat rectangular electrodes were fashioned. While the thickness of the electrodes varied slightly, they were constructed to have very nearly the same total surface area of 52 cm^2. The electrodes were fastened to a banana jack mounted in a plastic cup; the cup was then filled with fiberglass resin to insulate the connection from the sea water. This arrangement made it easy to change electrodes during the experiments and allowed the use of the same cables for each experiment. The resistance of each banana connection was measured and found to be negligible in comparison to the electrode resistances.

Upon completion of the ac tests, the platinum electrodes were plated in a solution containing 3g chloral platinic acid (H_2PtCl_6) with .2g lead acetate Pb $(C_2 H_3 O_2)_2$ in 100 ml of distilled water thus coating them with a film of "Platinum Black". This was done prior to completing the dc resistance and receiving impedance tests. Similarly upon completion of the ac tests, the silver electrodes were electrolyzed in a weak solution of hydrochloric acid (HCl), coating them with a film of silver chloride. The ac, dc, and receiving impedance tests were then conducted using the silver silver-chloride electrodes. Figures 16 through 20 are photographs showing the equipment used in the experiments.

C. PROCEDURES

1. AC Impedance

The low frequency ac impedance of the electrodes was determined

using the circuit shown in Fig. 13. The output of a Wavetek (Model 186) low frequency signal generator was monitored using recorder A, a Mark 220 Clevite Brush recorder, and was fed to the electrodes in the tank through a one ohm resistor. The electrodes were positioned as shown, one meter apart. The voltage across the one ohm resistor was monitored using recorder B, a calibrated Varian F-100 pen recorder. The recorders were found to be convenient for the low frequencies used in the tests. The voltage across the one ohm resistor indicated the total current in the electrodes. Peak-to-peak voltages and currents were used throughout the computations. The peak-to-peak output of the signal generator was adjusted to provide a measureable current through the one ohm resistor and, once adjusted, was held constant for all frequencies. The drive voltages required for good current readings varied between 5 mv and 200 mv, depending on the resistance of the electrodes being tested. The ac measurements were made in increments of 0.1 hertz for 0.1 to 1.0 hertz. The actual frequencies, which varied slightly from the above, were determined from the recordings.

2. DC Resistance

The dc resistance measurements were made using the circuit shown in Fig. 14. The electrodes were connected to the dc output of the Wavetek signal generator through the one ohm resistor. The voltage across the electrodes was monitored with voltmeter A, a Hewlett Packard model 419A dc null voltmeter. The voltage across the one ohm resistor was monitored with voltmeter B, a CIMRON model DMM51A, five place digital voltmeter.

The signal generator was adjusted to provide approximately four volts dc across the electrodes, the system was then allowed to settle

and the voltage across the one ohm resistor was recorded. The output of the Wavetek was then stepped incrementally to zero with the system being allowed to stabilize at each step before recording the voltage across the resistor. The resistor voltage was then converted to current, and voltage versus current plots made for each electrode pair. Four volts was found to be about the maximum voltage which could be applied across the electrodes without exceeding the work function of the materials concerned, which if exceeded, would drastically alter their resistive characteristics.

3. Receiving Impedance

Receiving impedance tests were conducted on the silver, platinum, carbon, and zinc electrodes using the circuit shown in Fig. 15a and b. The tests were designed to measure the open-circuit voltage and short-circuit current across the electrodes produced by an external E field.

Figure 15a shows the circuit used to measure the open circuit voltage across the electrodes. Electrodes A and B, standard laboratory silver, silver-chloride electrodes, were connected across the Wavetek to produce the horizontal E field in the tank. They were positioned 150 centimeters apart, as shown in the diagram, and the voltage across them was monitored on the X axis of the Varian pen recorder. The receiving electrodes C and D were positioned 50 centimeters apart, centered between the transmitting electrodes, and connected to the Y axis input of the Varian recorder. The output of the signal generator was adjusted to provide a measureable signal at the receiving electrodes, about 100 mv peak-to-peak, and a graph of transmitted voltage versus received open circuit voltage was plotted on the Varian recorder. Plots were made at 0.05, 0.1, and 1.0 hertz for each of the four electrodes pairs. The

phase angle between the transmitted and received voltages was determined using standard Lissajous pattern techniques [Michels 1957].

To measure the short-circuit current the circuit shown in Fig. 15b was used. A one ohm resistor was placed across the electrodes and across the Y axis input to the Varian recorder. The voltage across the one ohm resistor is equal to the current flowing through it. The Y scale on the recorder was adjusted to present a measureable reading and plots of transmitted voltage versus received current were made for the same frequencies as above. The current through the one ohm resistor is a good approximation to the short-circuit current, when the impedance of the electrodes is greater than 10 ohms or so, a condition very nearly always satisfied in these experiments.

The ratio of the quotients of received voltage (E_r) and transmitted voltage (E_t) to quotients of received current (I_r) and transmitted voltage were taken for each frequency to give the receiving impedance

$$\frac{E_r/E_t \angle \phi_1}{I_r/E_t \angle \phi_2} = \frac{E_r}{I_r} \angle (\phi_1 - \phi_2) = Z_r \angle \phi_r \quad .$$

The receiving impedance gives a relative measure of the electrode system's ability to detect horizontal E-fields.

D. DATA

The experimental results are presented in Figs. 21 through 46 and summarized in table 3. Figures 21 to 34 are graphs showing the ac resistance versus frequency of each of the electrode pairs. The values of ac impedance on the graphs are normalized by multiplication by the square root of the surface area of the electrodes, hence the unit ohm-meters.

Although the graphs of the hard metals appear exponential, the relation is not a simple one. The curves were plotted on log-log graph paper and the results in all cases were fairly linear. The function which best fits the data was determined using a least mean squares linear regression on the log-log plots and is given on each of the impedance versus frequency graphs.

The softer materials tested: tin, lead, and aluminum show altogether different characteristics than the others. These materials were extremely active in the sea water and low voltage tests were very difficult. Small differences in surface composition of these electrodes created battery-like conditions which caused large signal fluctuations.

Figures 35 to 46 are graphs showing dc voltages versus current for each electrode pair except titanium. DC resistance could not be obtained for titanium without using exceedingly high voltages, and it is therefore not included in the data. The values of dc resistance given in table 3 are the slopes of these curves normalized with respect to surface area. Where two separate slopes were observed both resistance values appear in the table and are labeled'High Voltage' and 'Low Voltage' resistance.

Figure 47a, b, and c are examples of the Lissajous patterns used to determine Z_r, the receiving impedance. The values determined from these plots appear in table 3 along with the phase angle ϕ_r.

The receiving impedance tests show a capacitive reactance component in the electrode impedance. The results of the test indicate that silver and plantinum electrodes have a much smaller reactive component than zinc and carbon. This observation was checked against low frequency voltage versus current traces on the oscilloscope where similar patterns

Material/f	High Voltage (dc)	Low Voltage (dc)	.1 Hz	.5 Hz	1.0 Hz
Silver	1.34	11.88	8.15	2.74	1.91
Silver Silver Chloride	1.997	3.75	.397	.375	.363
Aluminum	.921	14.76	155.75	238.83	238.83
Carbon	1.306	2.041	1.10	1.08	1.0
Copper	1.089	5.072	3.0	2.15	1.8
Nickel	.914		313.16	95.35	56.66
Lead	7.947	7.947	50.97	52.27	52.27
Platinum			7.875	5.653	4.822
Platinum Platinum-Black	.579	3.14	.847	.761	.761
Tin	.869	16.24	71.82	63.13	44.7
Stainless	.963	10.67	31.35	10.33	6.88
Titanium			203.66	49.0	27.3
Tungsten	21.17	127	60.24	21.58	12.86
Zinc	.979	1.91	3.14	2.09	1.75

Table 3 Z vs f

	.05 Hz		.1 Hz		1.0 Hz	
	$\|Z\|$ Ω	$\phi°$	$\|Z\|$ Ω	$\phi°$	$\|Z\|$ Ω	$\phi°$
Silver Silver-Chloride	50.12	- .75	49.1	- 3.47	55.88	- 2.32
Platinum Platinum-Black	6.8	-13.63	5.97	-12.65	5.43	- 8.97
Carbon	22.61	-43.29	16.65	-36.16	11.63	-18.21
Zinc	22.73	-31.32	26.85	-38.51	13.83	-33.68

Table 4 Receiving Impedance Z vs f

were observed. There is however, insufficient recorded data at present to make any quantitative estimate as to the manner in which the capacitance changes with frequency. Factors, such as the geometry and spacing of the electrodes as well as the size and shape of the tank are believed to have a marked effect on the capacitance and it is therefore recommended that further tests of this phenomenon be conducted either at sea or in a larger tank with greater spacing of the electrodes.

IV. DISCUSSION

A. ELECTRODE IMPEDANCE

The results of the experiments described in the preceding section clearly show that based upon electrode resistance either platinum platinum-black or silver silver-chloride electrodes are superior to the others tested. Copper, zinc, and carbon also have relatively low resistance and could be considered. Copper, while having a fairly low resistance, was found to be difficult to work with. The oxidation which formed on the copper electrodes in the salt water was extremely delicate and would slough off, causing sharp resistance changes during the tests. Although all of the materials were found to form oxidation on their surfaces during the tests, only those on copper, zinc, and silver appeared to cause radical changes in the resistive behavior of the electrodes. The exact mechanism of these changes is not clearly understood, however there is a possibility of two separate effects. The first effect appears to be an increase in surface area. This is especially visible in the platinum platinum-black electrodes. After platinizing, the surface is extremely granular and rough. This roughness, depending on its molecular nature, could increase the total surface area appreciably over the smooth surface. The decrease in the polarization effect (change of resistance with frequency) described in section 2 of this paper, is very apparent on the graphs of both the silver silver-chloride and platinum platinum-black. This reduction can be explained by the increased surface area of the electrodes, because for an increase in surface area there is a decrease in current density as well as a decrease in the ion

cloud density for a given potential. This may also, in part, explain the fact that very little polarization effect was observed in carbon. Earlier tests had indicated that carbon displayed a high degree of polarization and table 1 also shows a definite polarization effect for carbon. The difference may lie in the type of carbon used. In earlier tests, round, smooth, hard carbon rods were used as electrodes. In later tests, flat, porous carbon bars were used. The porosity of the carbon used in the later tests may have effectively increased the surface area in the same manner as the platinizing did to the platinum. If this is the case, use of the proper grade of carbon could provide a good electrode for considerably less cost than either platinum or silver.

A second possible mechanism by which the coatings may reduce the polarization effect is by formation of a screen that allows penetration of the electron but holds the ions far enough away from the surface of the metal to preclude the cloud formation. This mechanism, however, does not explain the behavior of carbon. It is believed that both of these mechanisms are present, and play some roll in the reduction of resistance.

The materials which show strong polarization characteristics such as tungsten, titanium, stainless steel, and nickle all have extremely hard smooth surfaces. The surfaces of the platinum and silver electrodes were also smooth and hard prior to coating, as they were cold rolled into the desired thickness and had experienced some strain hardening. Since the polarization effect appears to be associated with the surface characteristics of the electrode, other methods of reduction could be tested, such as machine roughening or acid etching, to determine their effects on resistance.

The coatings formed on silver, platinum and zinc, while not as delicate as that formed on the copper, did require careful handling. If another method could be found which produces the same results, it could greatly simplify the task of deployment and recovery of an actual antenna.

B. ANTENNA DEPLOYMENT

Deployment and recovery of loop antennas and short rigid dipoles up to several meters in length have been successfully completed on board the R/V ACANIA. Deployment and recovery of a non-rigid, long-wire electric dipole on the order of several hundred meters in length however poses special problems. If the wire connecting the electrodes is not laid straight or nearly so, the actual distance between electrodes is not known and the E field cannot be exactly determined. Also, if there are any loops formed in the connecting wires, unwanted voltages may be introduced adding to system noise.

During the fall of 1978, a 100 meter dummy antenna was successfully deployed and recovered in 150 feet of water in Monterey Bay from the R/V ACANIA. The method of rigging is shown in Fig. 47. The antenna electrodes were connected 100 meters apart to a length of 3/8 inch polypropylene line. The wire connecting the electrodes together was 105 meters of RF 58 shielded cable. The wire was then attached to the polypropylene line at several points, allowing enough slack in the wire to ensure it came under no strain, but not enough slack to cause looping of the wire. One end of the polypropylene line was then bouyed, the electrode at the opposite end was affixed rigidly to a weighted pressure vessel designed to carry the instrumentation package. The pressure vessel was connected to the ship's winch with 600 feet of

one inch nylon line. The bouyed end of the antenna was placed in the water and the antenna was streamed out on the desired heading. When the antenna was fully streamed, the instrument package was lowered just below the surface. The small boat from the ship then proceeded to the bouyed end of the antenna and replaced the bouy with a five pound weight. Simultaneously the ship began lowering the instrument package with the other electrode, while steaming dead slow on the desired heading, until the instrument package reached the bottom. Retrieval was accomplished by hauling the instrument package on board and disconnecting the electrode, then retrieving the antenna wire and other electrode by means of the attached polypropylene line. Upon recovery the antenna system was inspected for damage and none was found. It is anticipated that this system can be used for longer antennas and greater depths, as long as the bottom is smooth sand or clay. In rocky or rough bottoms there is a possibility of fouling the outboard electrode and causing damage.

C. ELECTRODE NOISE

As mentioned in section 2 of this paper, the main source of antenna noise appears to be caused by water motion across the surface of the electrode. It is theorized that this noise is due to a disturbance of the polarization or ion cloud surrounding the electrode. If this is correct, then the choice of electrode material could greatly affect the noise of the system. In addition to proper choice of material, some form of electrode covering has been found to be necessary to prevent the water from moving directly across the surface of the electrode, while allowing free contact of the electrode with the water. Wrapping the electrode in several layer of gauze has proven successful, however,

after several hours of use the gauze shows a tendency to build up polarization and thereby increase the resistance of the dipole [Strarup 1966]. The thickness of the gauze used must therefore, be a compromise between the maximum allowable resistance and the amount of noise which can be tolerated.

Observations were made in the laboratory using a porous polypropylene vacuum pump filter to cover the silver silver-chloride electrodes. There was no apparent change in the resistive or polarization characteristics of the electrodes. Noise measurements were not conducted during the experiments reported here, however, it is recommended that the polypropylene filter be tested as a noise reduction measure when such tests are accomplished.

It is recommended that the silver silver-chloride, platinum platinum-balck, carbon, and zinc electrodes be tested further, either in a larger tank or at sea to determine the exact nature of their capacitive characteristics, the effects of electrode geometry on the total impedance, and to further investigate various means of water noise reduction.

APPENDIX A

Antenna	E_{oc}	I_{sc}	G_R	V_{NM}
Dipole	ℓE	$\frac{\ell E}{R_w + 2R_e}$	$\frac{4 k^3 \ell \delta^2}{\pi}$	$\ell \frac{ds}{dt} B \sin \phi$
Loop	$-J\omega N A_L B$	$\frac{-J\omega N A_L B}{R_w + J\omega L_L}$	$\frac{3 k^3 a \delta^2}{4}$	$N A_L B \sin \phi \frac{d\Phi}{dt}$

Table 5

To compare the loop and dipole antennas the following assumptions are made: (i) Both antennas are immersed in a semi infinite conducting medium. (ii) The electromagnetic field to be measured eminates in free space above the boundary. (iii) Below the boundary, both the electric and magnetic fields are horizontal. (iv) The plane of the loop antenna is vertical and perpendicular to the H field, the axis of the dipole is horizontal and parallel to the E field.

Table 5 summarizes the dipole relationships of section 2 and gives the corresponding relation for the loop antenna where:

N = number of turns

ω = signal frequency

A_L = area of loop

B = magnetic flux density

L_L = inductance of the loop

a = radius of the loop

The subscripts L and D will be used to denote loop and dipole respectively.

A. OPEN CIRCUIT VOLTAGE

Comparison of the open circuit voltage (E_{oc}) for the loop and dipole antennas requires expressing the electric field strength (E) in terms of the magnetic flux density (B). As a first approximation and neglecting displacement currents,

$$E = \frac{B}{\mu_o} \eta$$

where η is the complex intrinsic characteristic impedance of the conducting medium and is given as

$$\eta = \frac{j \mu_o \omega}{\gamma_1}$$

where $\gamma_1^2 = j \sigma_1 \mu_o \omega$ and σ_1 and μ_o are the conductivity and permeability respectively of the conducting medium. Substituting this into the above expression for E yields;

$$E = B \sqrt{\frac{\omega}{\mu_o \sigma_1}} \angle \pi/4$$

disregarding the phase shift and using the values for sea water of $\sigma_1 = 4$ S/m and $\mu_o = 4 \pi \times 10^{-7}$ H/m obtains

$$E = 4.46 \times 10^2 \, B \sqrt{\omega}$$

and

$$E_{oc_D} = \ell \, E = \ell \, 4.46 \times 10^2 \, B \sqrt{\omega}$$

If a loop antenna with a radius of 1 meter were designed to have the same open circuit voltage as a 100 meter dipole, then

$$E_{oc_D} = E_{oc_L}$$

implies

$$\omega N A_L B = 4.46 \times 10^2 \ell B\sqrt{\omega}$$

and substituting a = 1 meter and ℓ = 100 meters yields

$$N = \frac{4.46 \times 10^4}{\pi \sqrt{\omega}}$$

at a frequency of 1 Hz

$$N = 5.7 \times 10^3 \text{ turns}$$

for a total wire length of 3.58×10^4 meters. If the same gauge wire is used for the loop and the dipole, the wire resistances (R_w) are directly proportional to length and

$$R_{w_L} = 358\ R_{w_D}$$

B. SHORT CIRCUIT CURRENT

The ratio of short circuit currents using the above conditions gives

$$\frac{I_{scD}}{I_{scL}} = \frac{V_{ocD}/(R_{wD} + 2R_e)}{V_{ocL}/(R_{w_L} + J\omega L_L)}$$

with $V_{ocL} = V_{ocD}$ and $R_{w_L} = 358\ R_{w_D}$,

$$\frac{I_{scD}}{I_{scL}} = \frac{358\ R_{w_D} + j\omega L_L}{R_{w_D} + 2\ R_E}$$

using spherical electrodes with a surface area of 1 m^2 and number 12 copper wire,

$$R_{wD} = .005\ \Omega$$

$$2\ R_E = \frac{2K}{\sqrt{S}} = .28\ \Omega$$

and

$$I_{scD} = \frac{1.79 + j\omega L_L}{.285} \quad I_{scL} \geq 6.28\ I_{scL}$$

C. RELATIVE ANTENNA GAIN

Taking the ratio of the relative antenna gains from table 5 yields:

$$\frac{G_{rD}}{G_{rL}} = \frac{(4\ k^3\ \ell\ S^2)/\pi}{(3\ k^3\ a\ S^2)/4}$$

from whence:

$$G_{RD} = \frac{16}{3}\frac{\ell}{a}\ G_{RL}$$

and substituting the values of ℓ and a used above

$$G_{RD} = 170\ G_{RL}$$

D. MOTION NOISE VOLTAGE

To compare the noise voltage generated due to antenna motion in the earths static magnetic field, it is assumed that the motion of the dipole is in the horizontal plane and perpendicular to the dipole axis, and the motion of the loop is angular about its horizontal axis. The motion of both antennas is periodic with angular frequency ω and amplitudes s_o and θ_o respectively.

The noise voltage generated in the loop due to the above motion is given by;

$$V_{NML} = N A_L B \sin \phi \frac{d (\theta_o \sin \omega t)}{dt}$$

Therefore

$$V_{NML} = \omega \theta_o N A_L B \sin \phi \omega t$$

from section II

$$V_{NMD} = \ell S_o \omega B \sin \phi \cos \omega t$$

If the dipole is allowed to have a maximum displacement of, S_o = 1 cm, the corresponding loop motion can be determined by equating the noise voltages which gives

$$\omega \theta_o N A_L B \sin \phi \cos \omega t = \ell S_o \omega B \sin \phi \cos \omega t$$

from whence

$$\theta_o = \frac{\ell S_o}{N A_L}$$

using ℓ = 100 m, S_o = .01 m, N = 5.7×10^3 and $A_L = \pi$ m^2 gives

$$\theta_o = 5.58 \times 10^{-5} \text{ rad.} = 11.5 \text{ sec of arc.}$$

E. WATER MOTION NOISE

Water moving across the surface of the antenna has been observed to generate noise in both antenna systems. In the case of the loop antenna the noise appears to be associated with turbulence in the water flow around the loop. Hydrodynamic vortices at or near the surface of the

antenna form current loops which cause the magnetic noise. Enclosing the loop in a non-conducting sphere or radome has been used to reduce this noise. The water motion noise in the dipole antenna was discussed in section II. The major difference between the loop and the dipole with respect to this noise is that an increase in sensitivity of the loop, either by increasing its size or adding turns, also increases its sensitivity with respect to this noise whereas with the dipole, an increase in sensitivity by lengthening the antenna has no effect on this noise and hence the signal-to-noise ratio is improved.

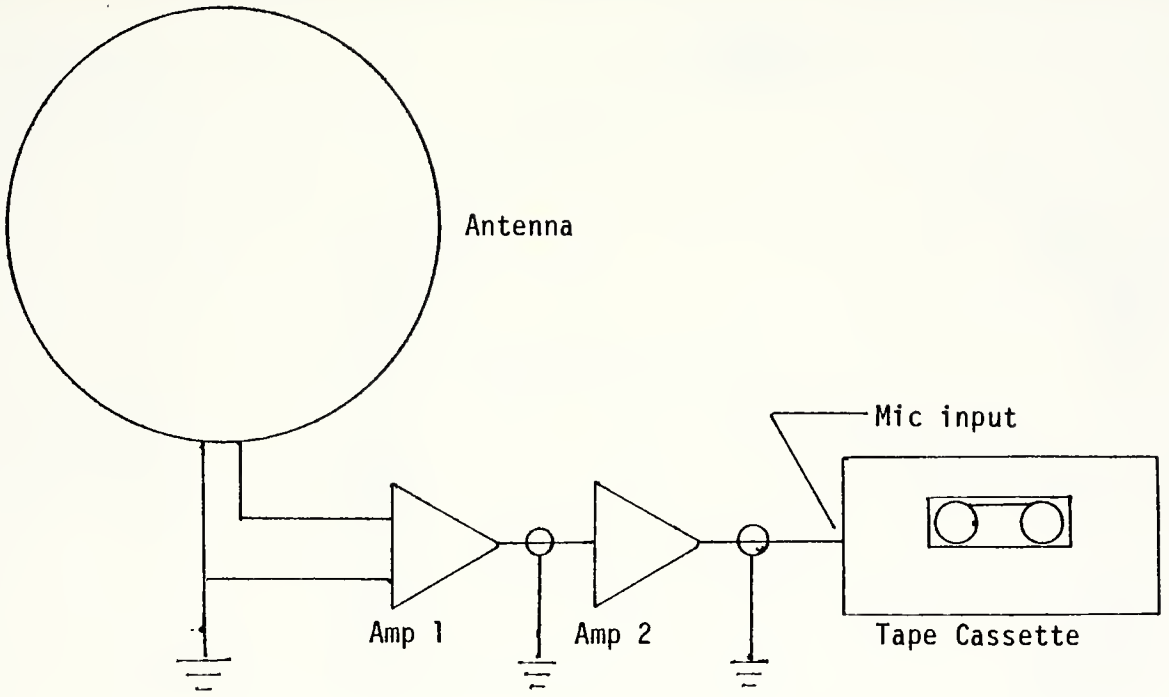

Fig. 1. Self-Contained Loop Antenna Electrical Configuration

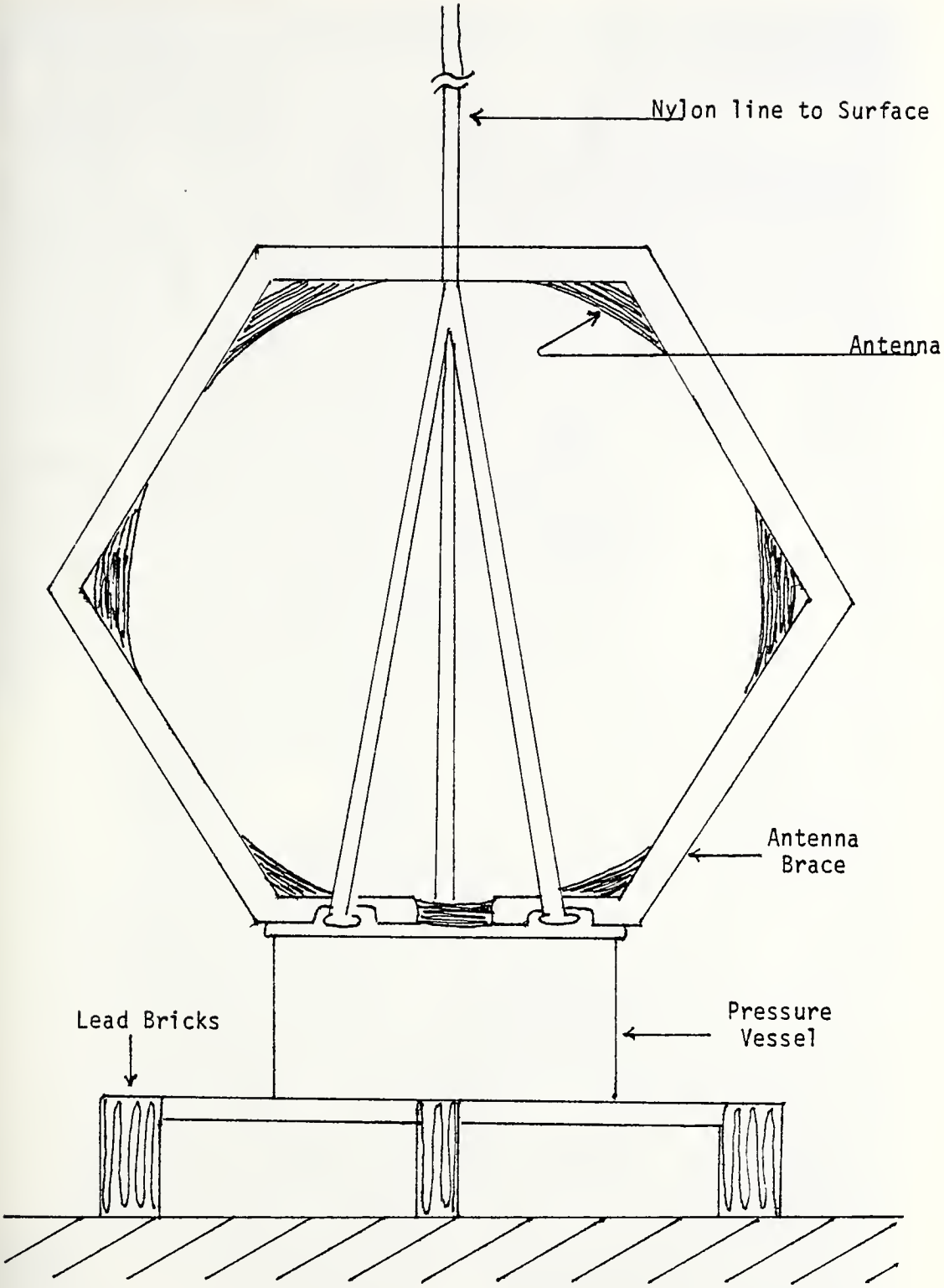

Fig. 2. Loop Antenna Mechanical Configuration

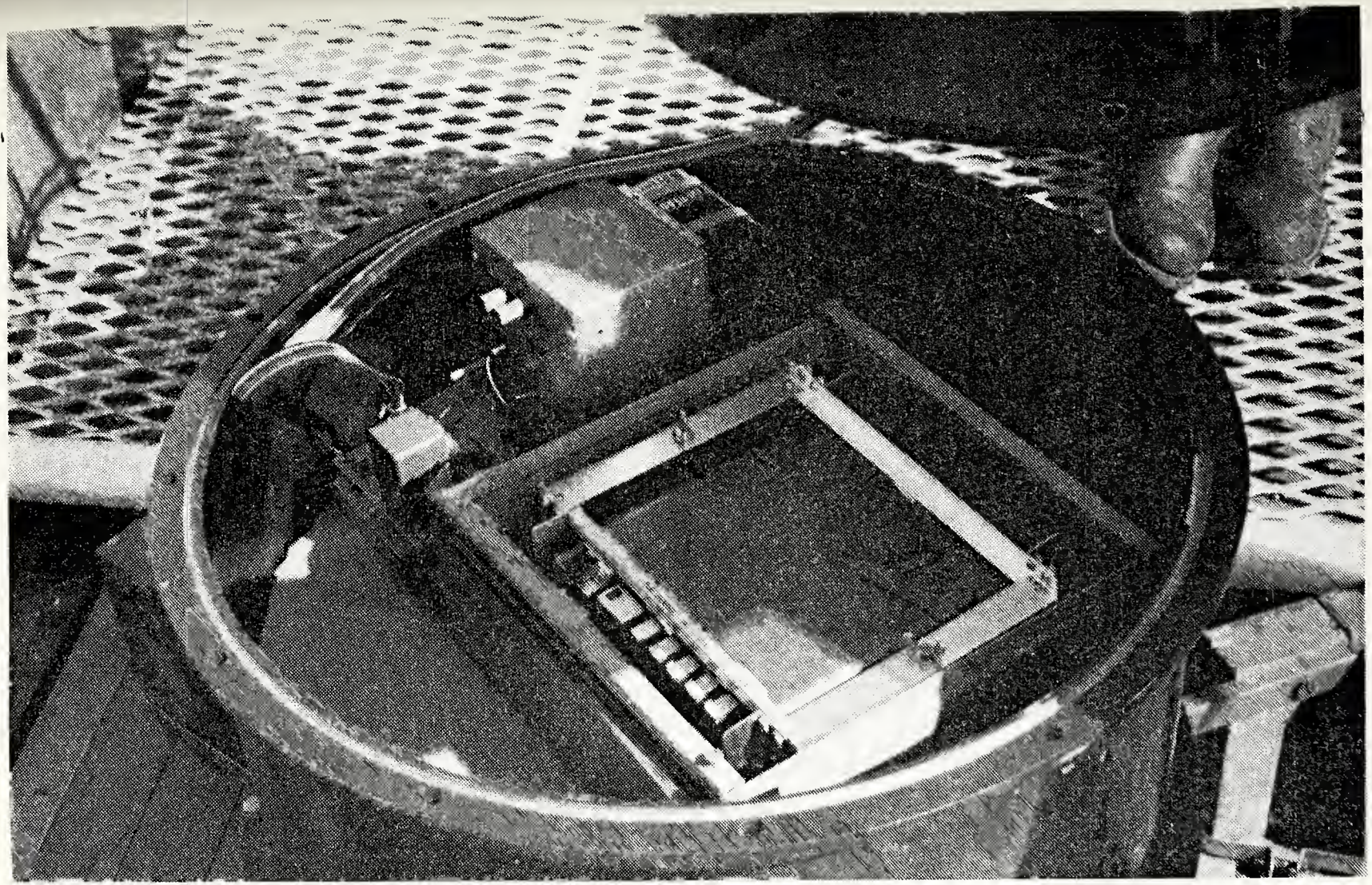

Fig. 3. Recorder and Amplifier in Pressure Vessel

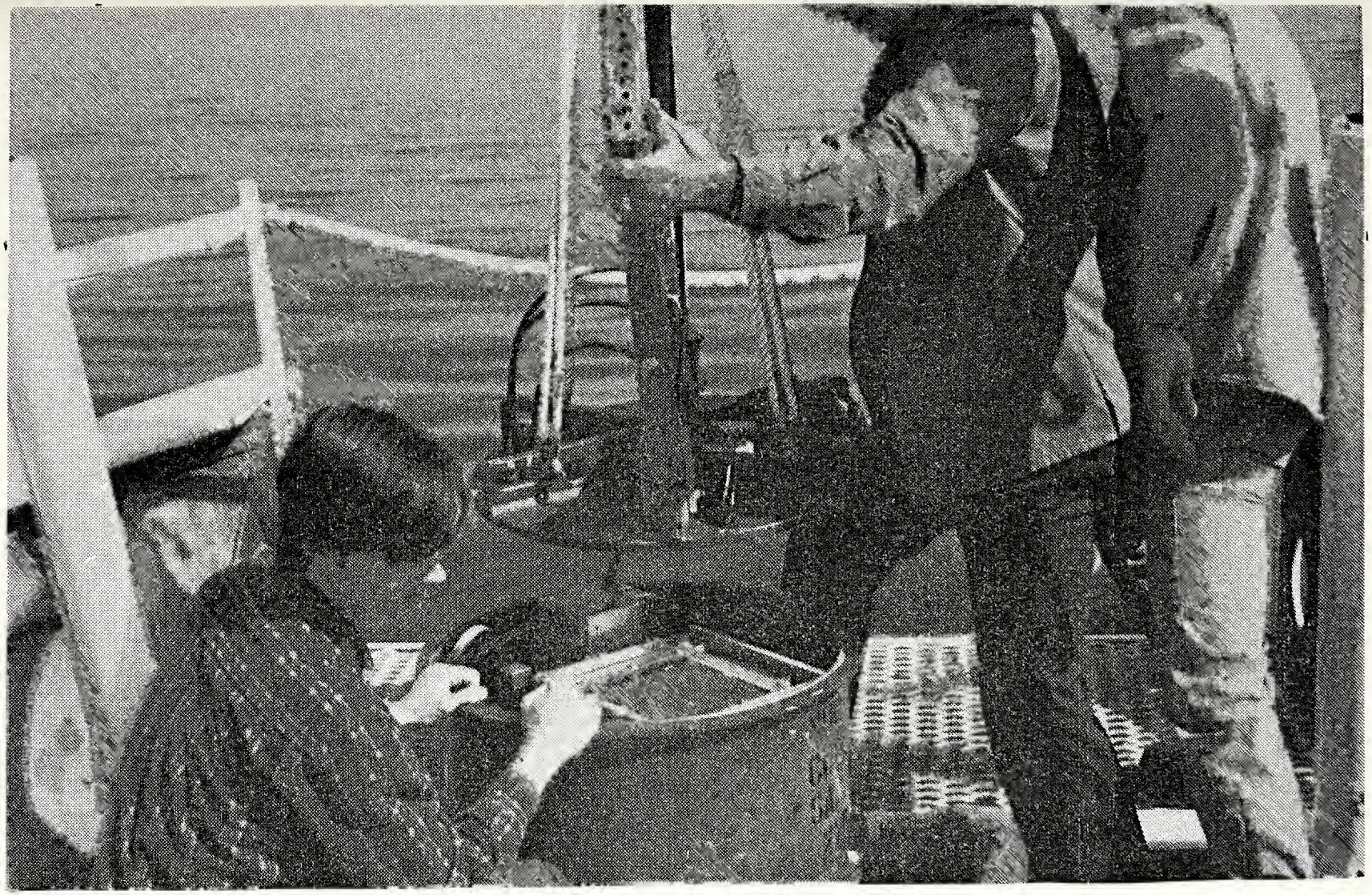

Fig. 4. Assembly of Antenna to Pressure Vessel

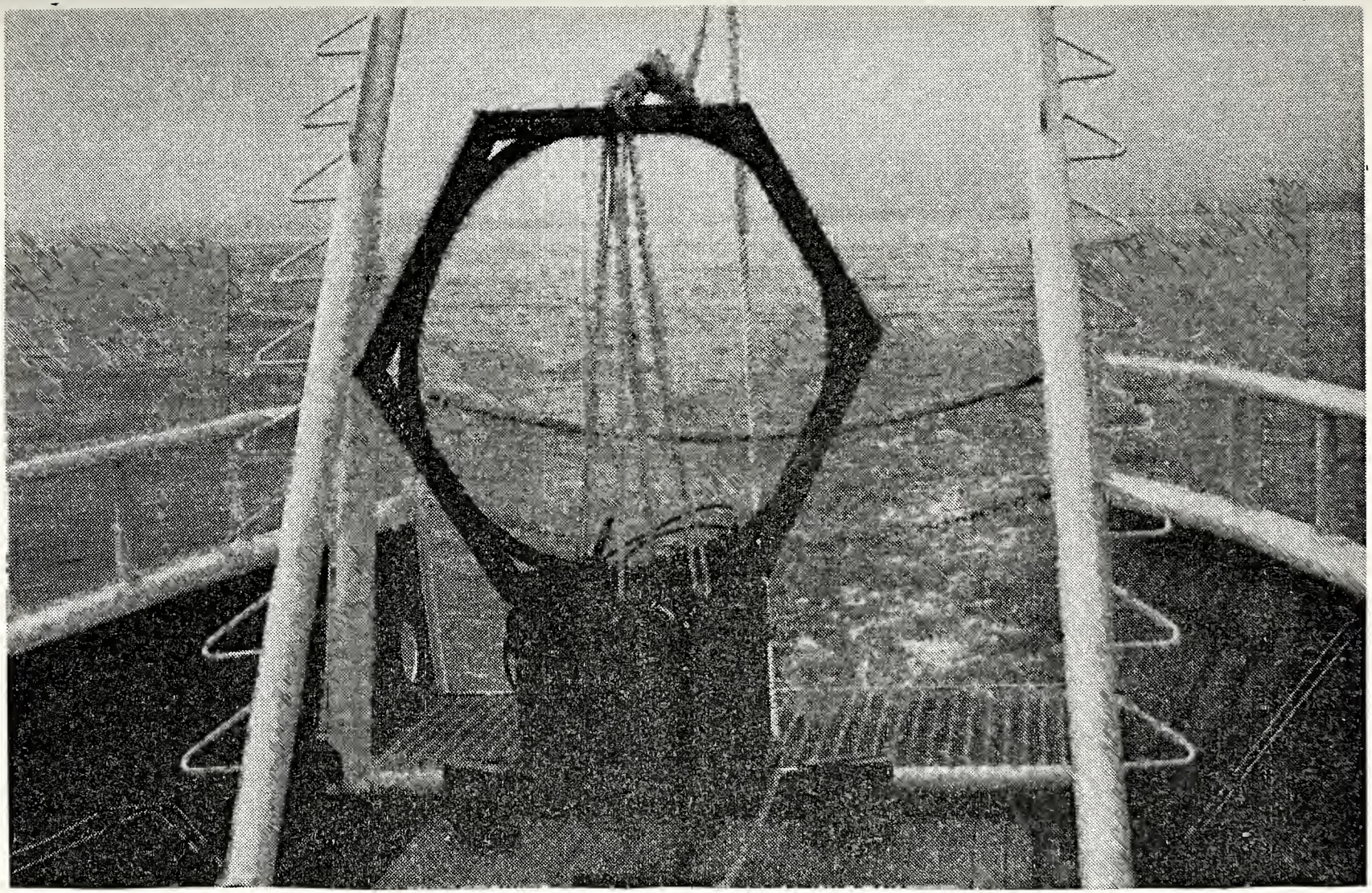

Fig. 5. Assembly ready for Deployment

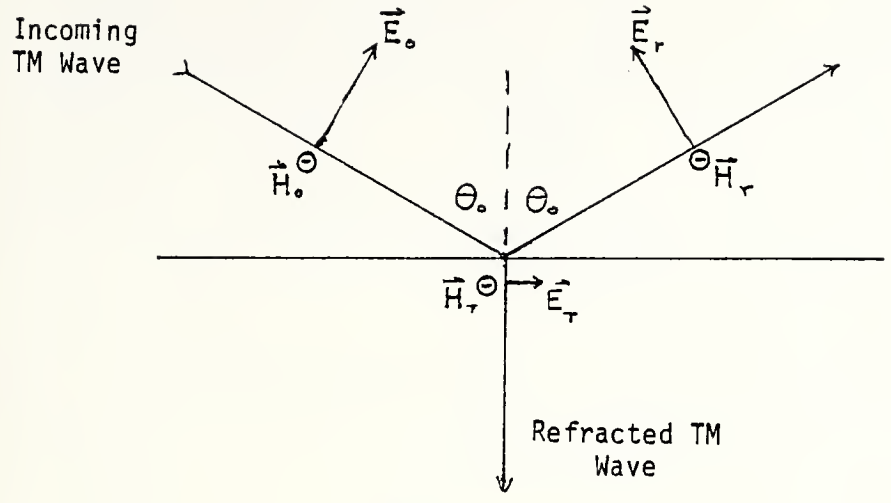

(a)

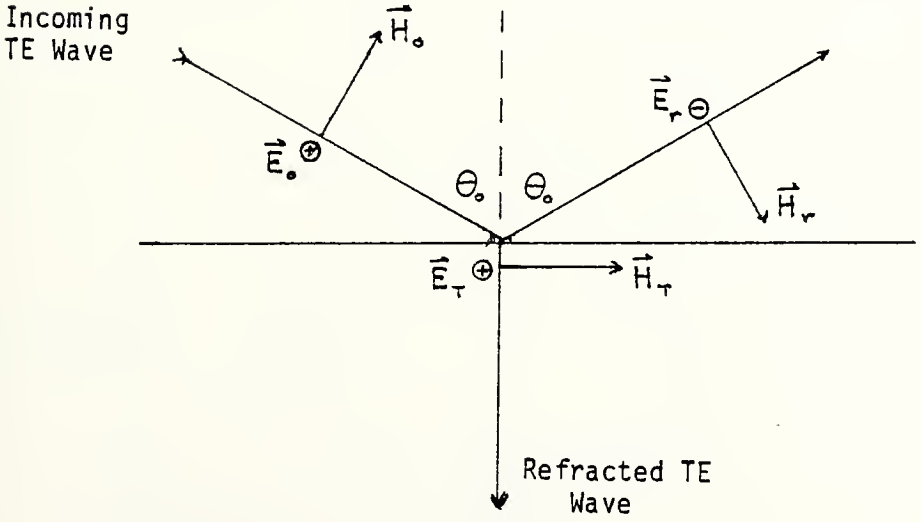

(b)

Fig. 6(a) TM Wave Refraction Diagram
(b) TE Wave Refraction Diagram

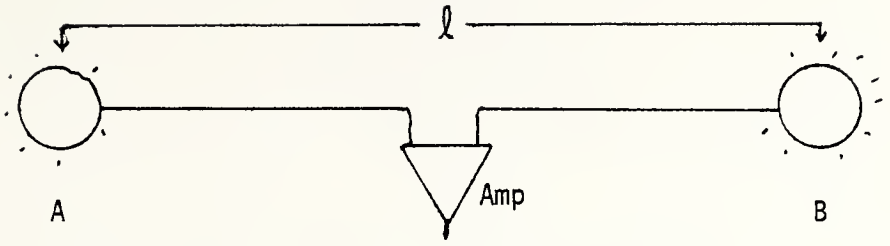

Fig. 7. Dipole Antenna

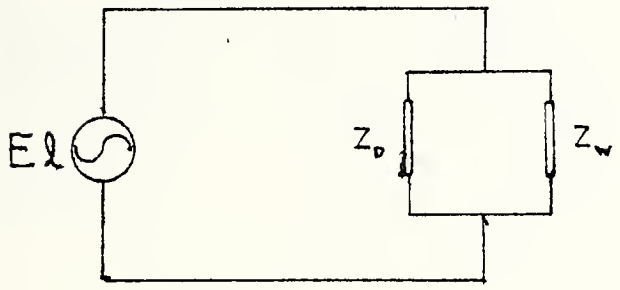

Fig. 8. Equivalent Circuit for Water and Antenna Impedances

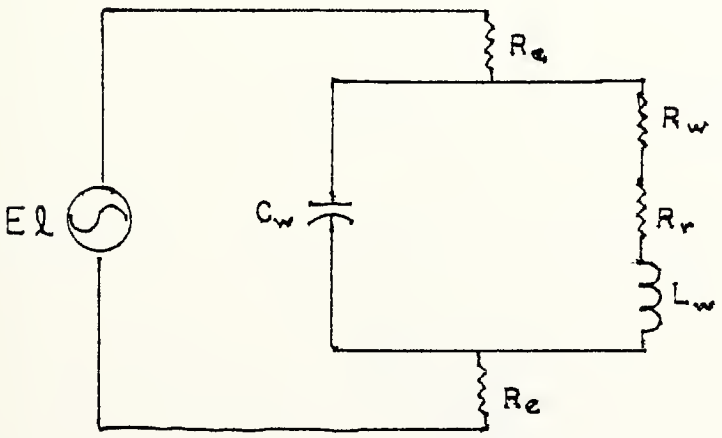

Fig. 9. Equivalent Circuit for Antenna Impedance

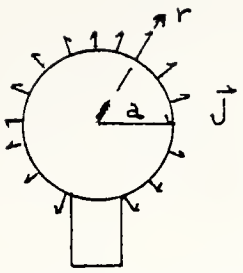

Fig. 10. Electrode as a Spherical Current Source

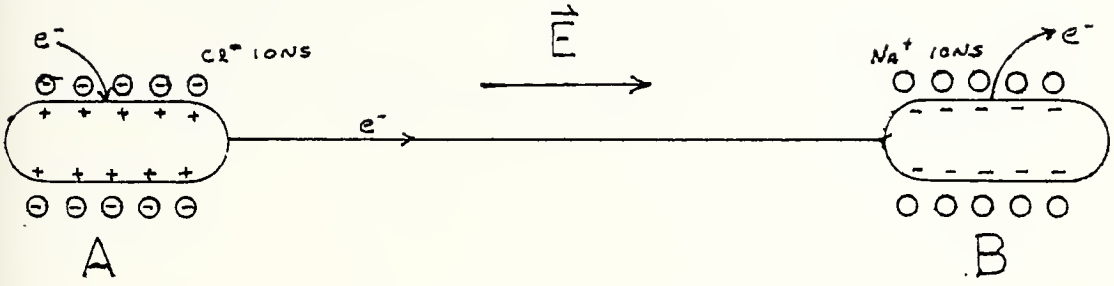

Fig. 11. Dipole Polarization Diagram

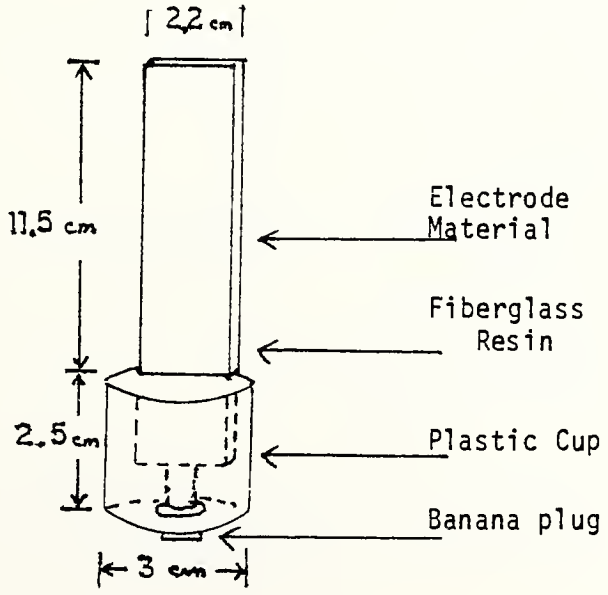

Fig. 12. Experimental Electrode Configuration

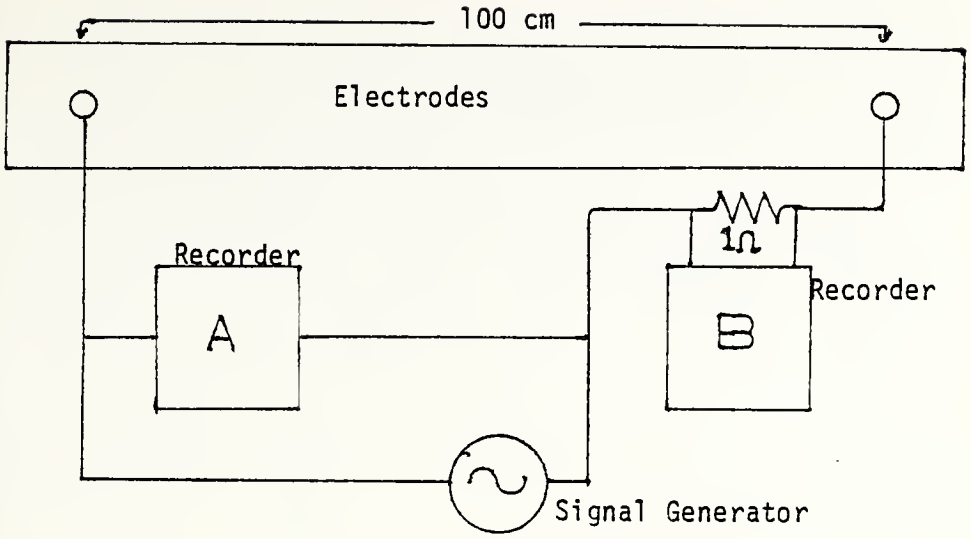

Fig. 13. AC Impedance Measurement Configuration

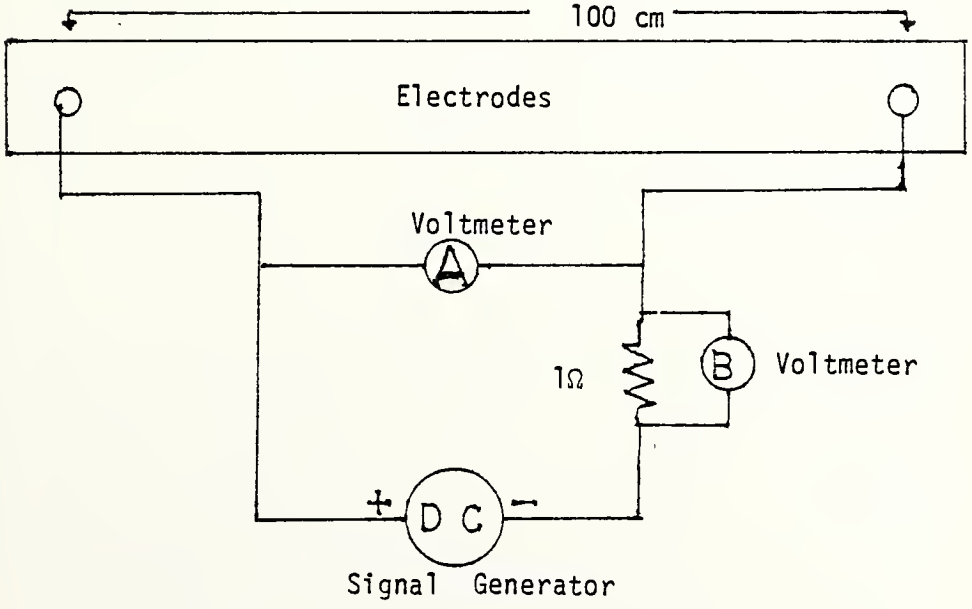

Fig. 14. DC Resistance Measurement Configuration

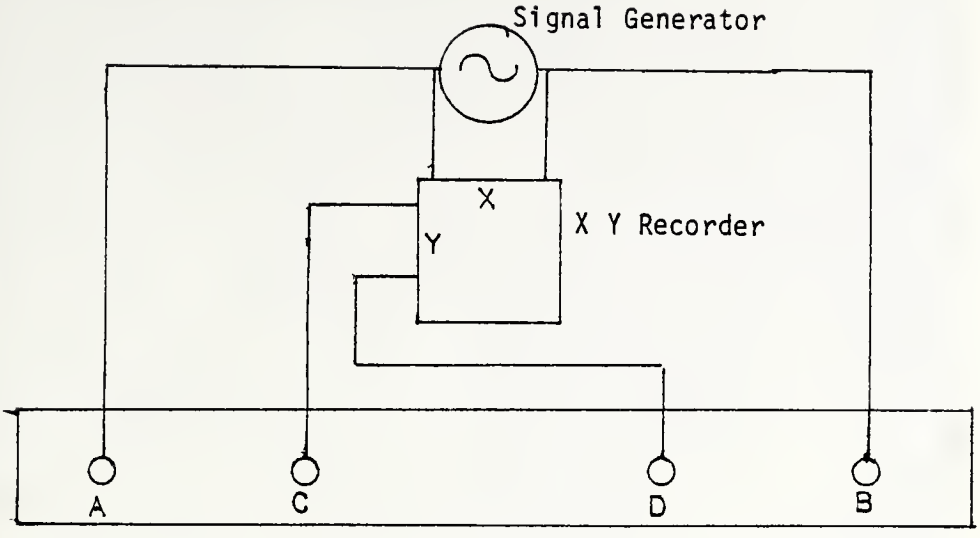

(a)

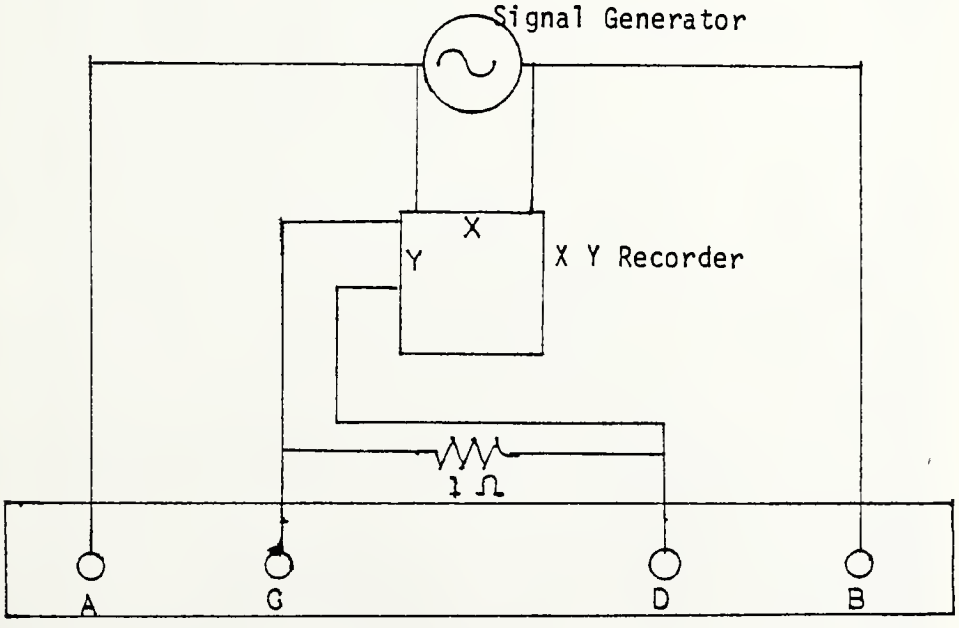

(b)

Fig. 15. Receiving Impedance Measurement Configuration
(a) Open Circuit Voltage
(b) Short Circuit Current

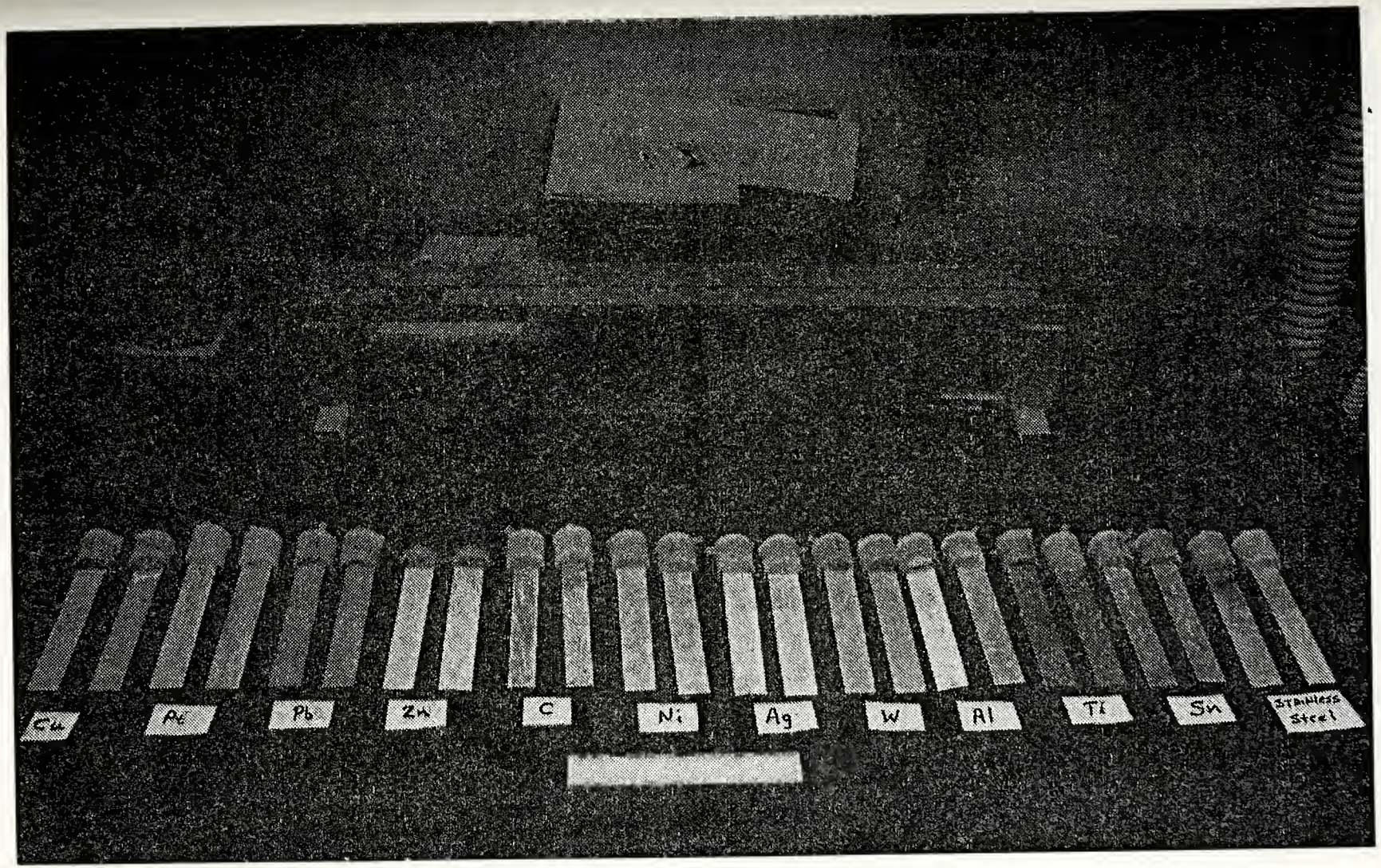

Fig. 16. Electrodes Used for Experiment

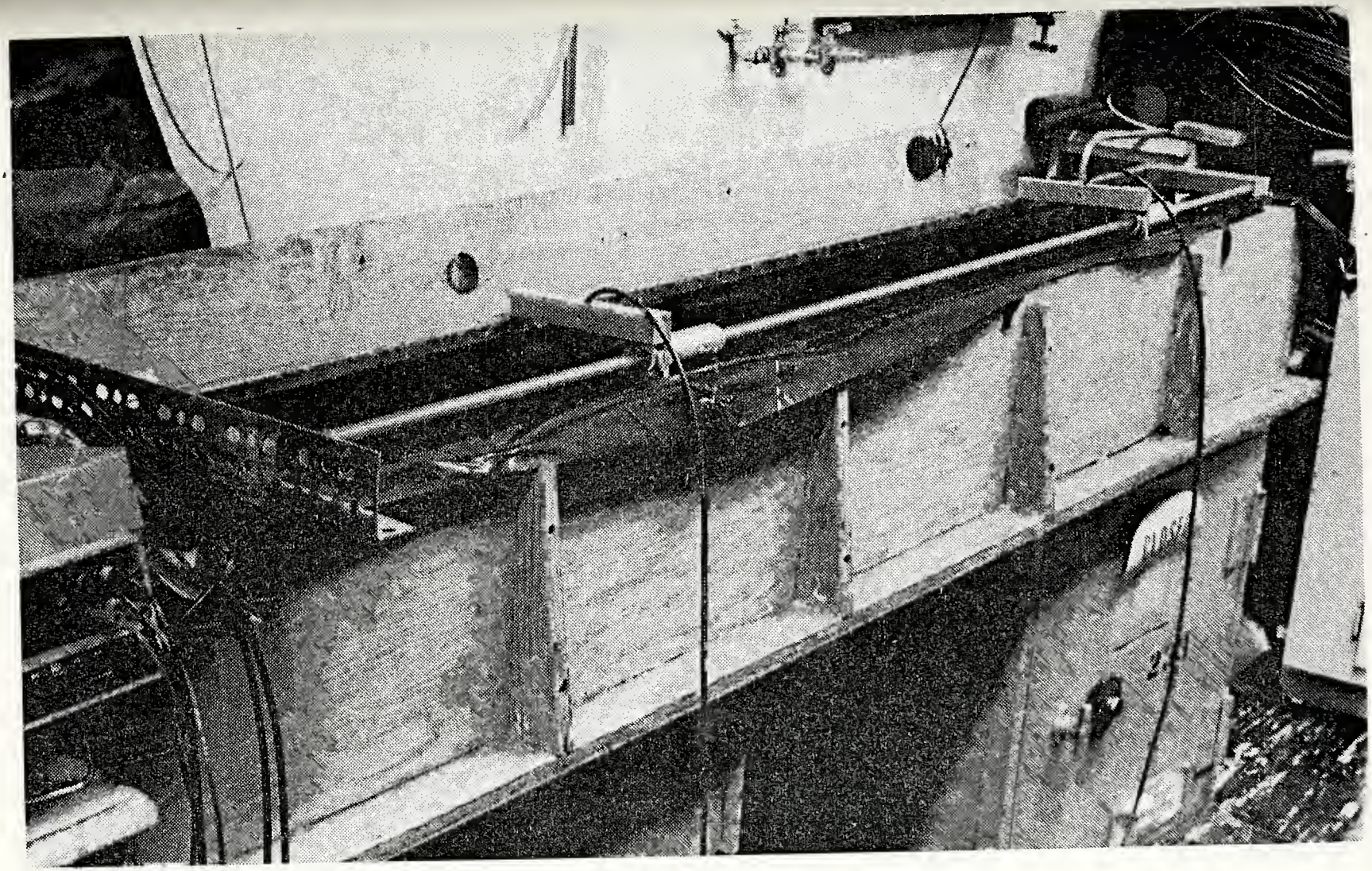

Fig. 17. Trough Used for Experiment

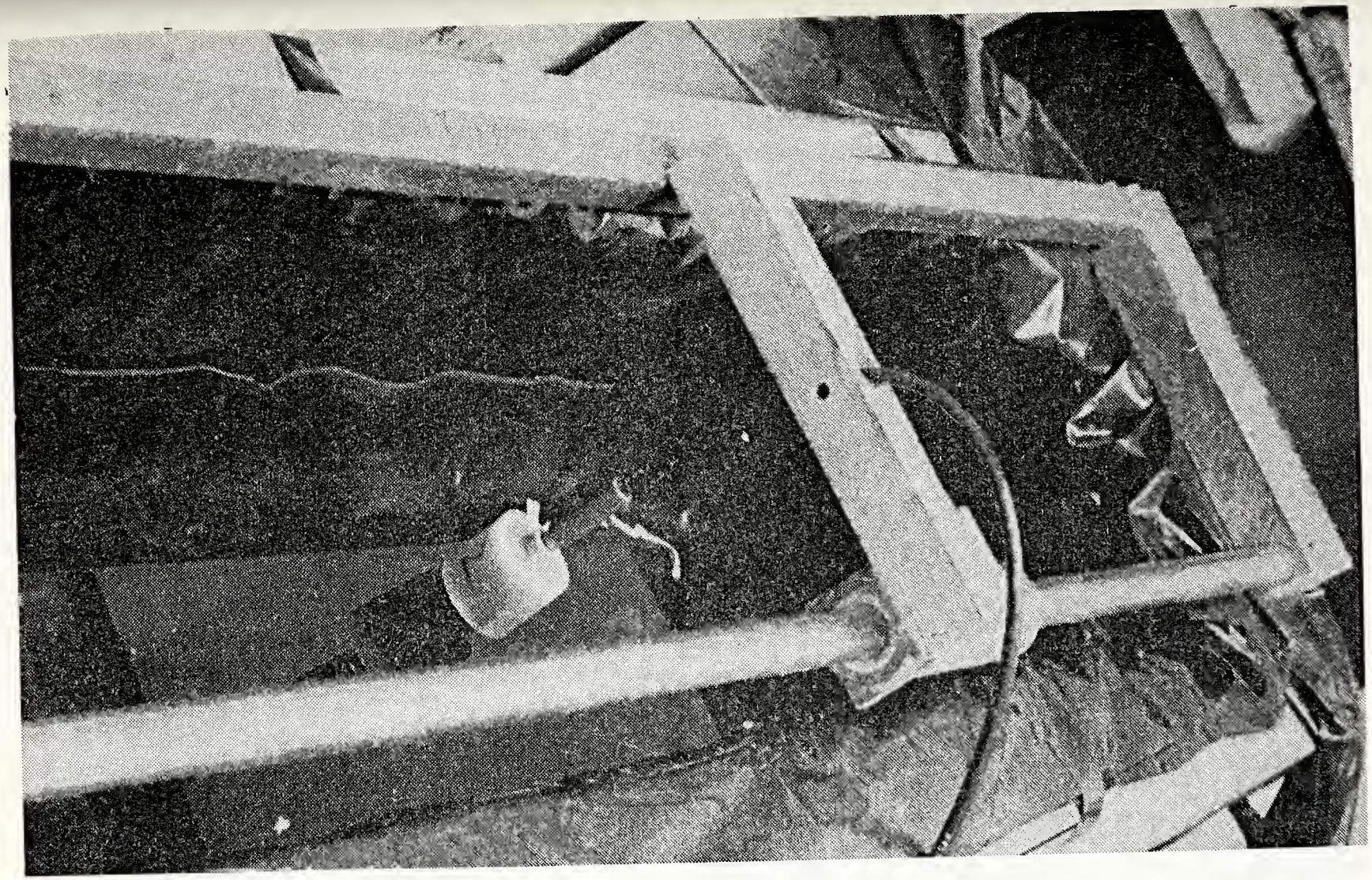

Fig. 18. Banana Jack Connection Technique

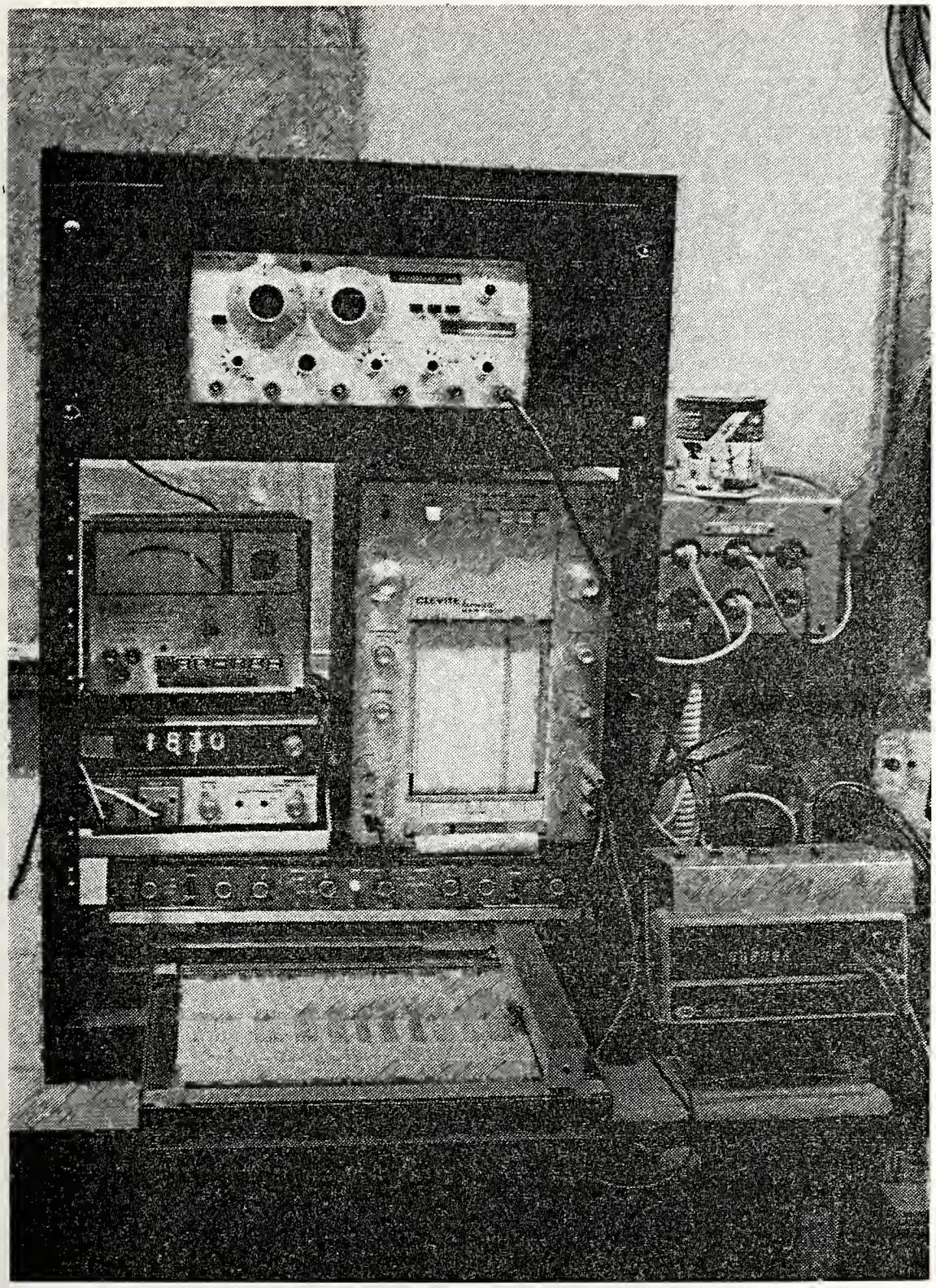

Fig. 19. Electronic Equipment Used in Experiments

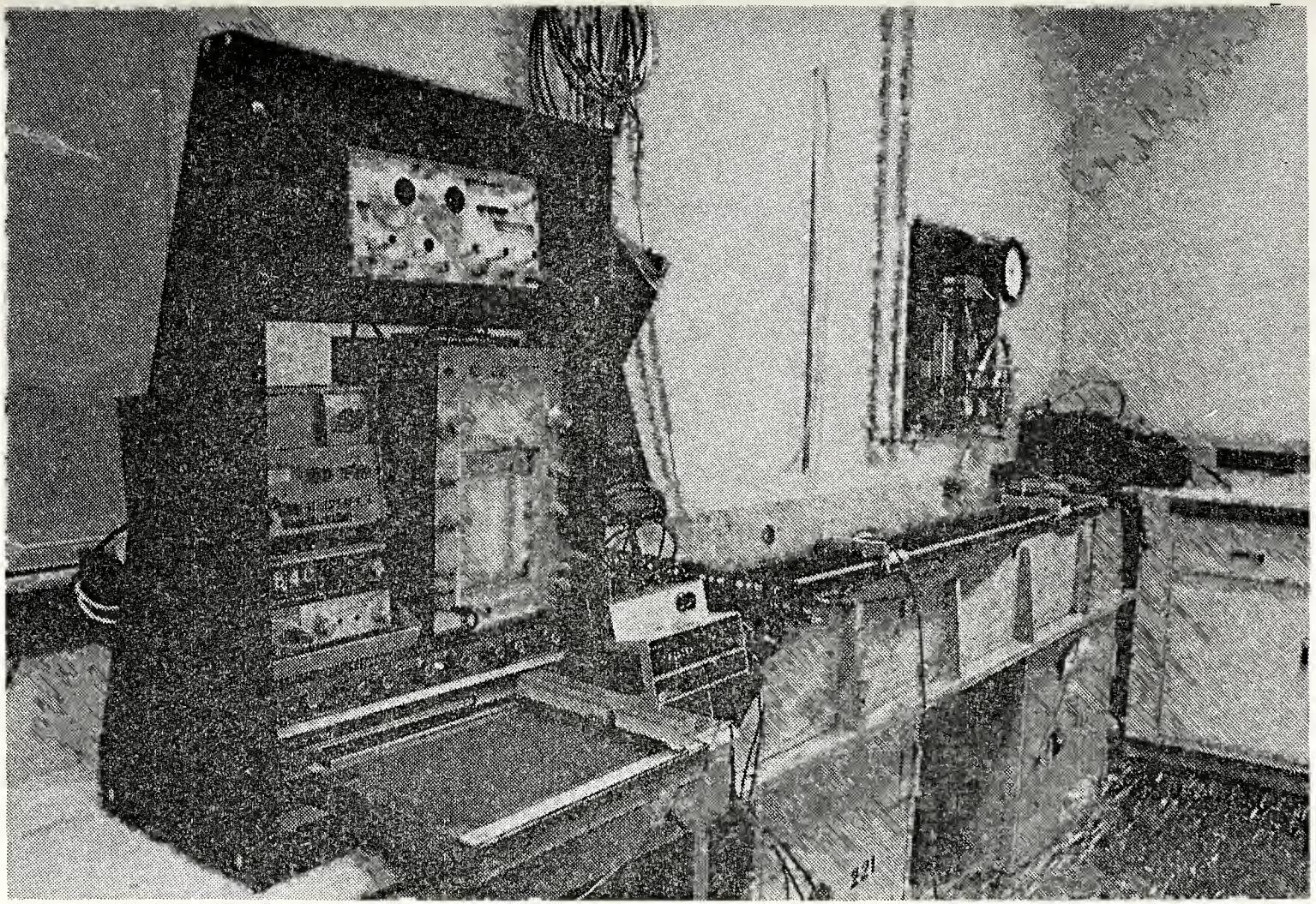

Fig. 20. Complete Experimental Apparatus

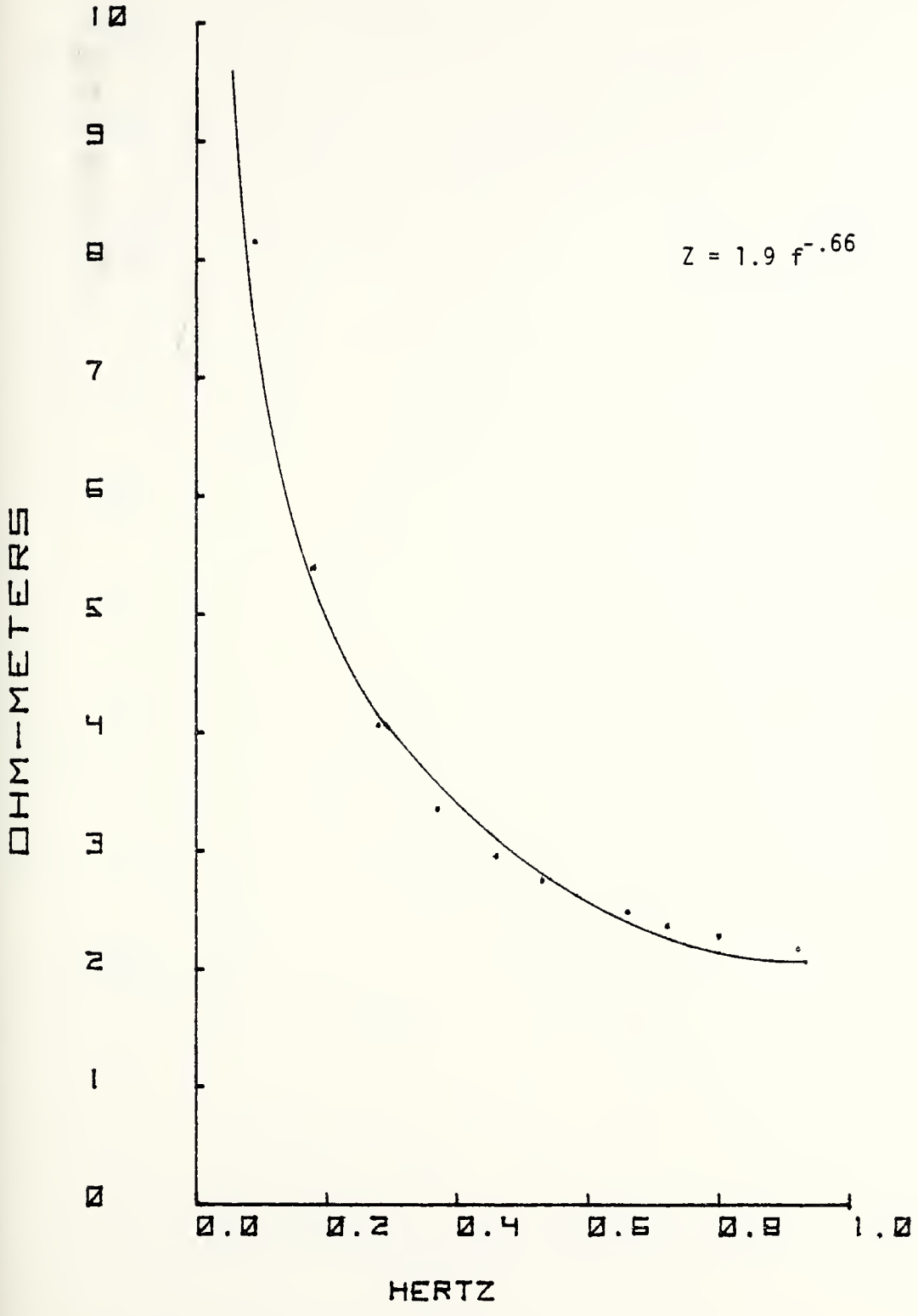

Fig. 21. Silver Z vs f

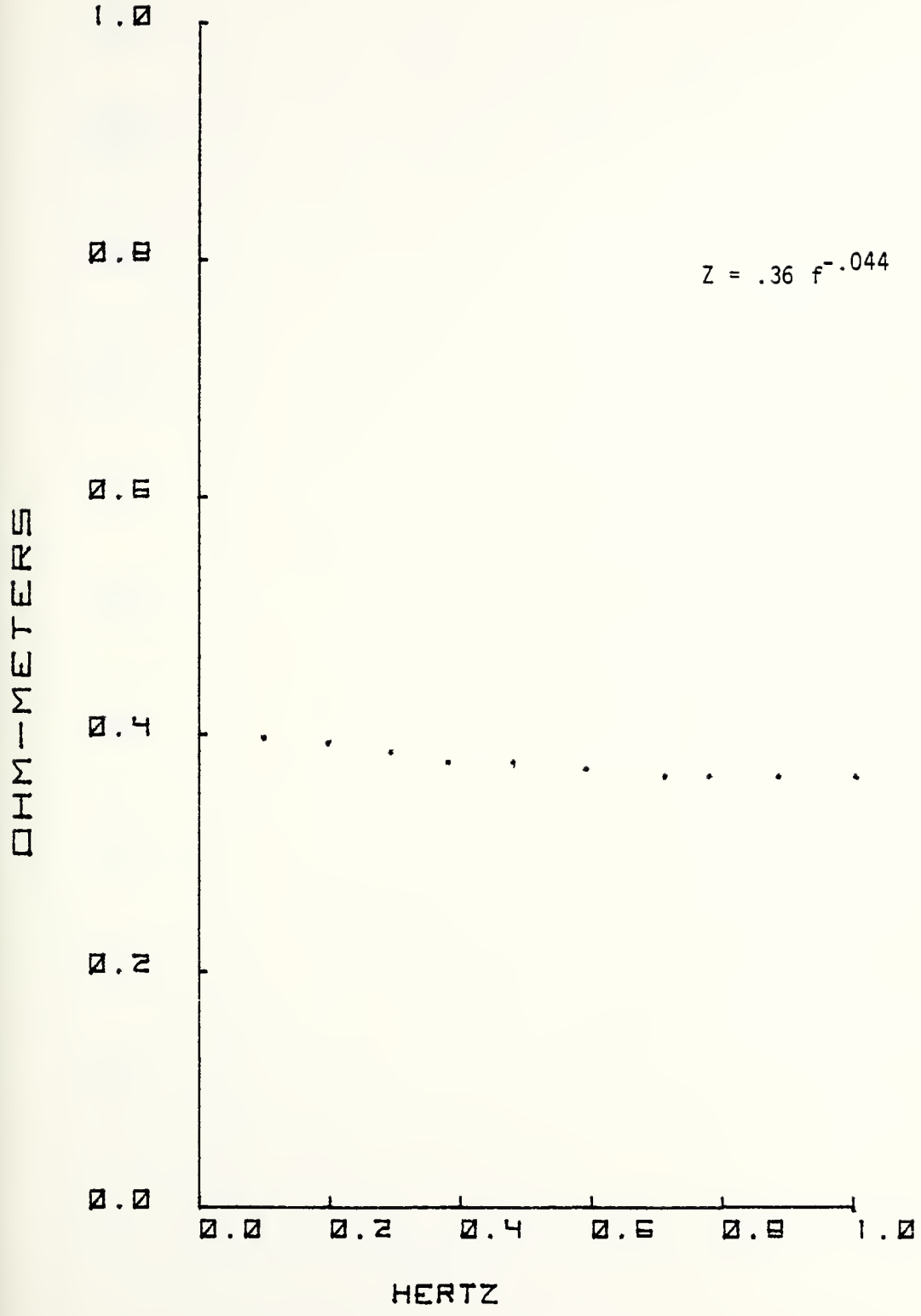

Fig. 22. Silver Silver-Chloride Z vs f

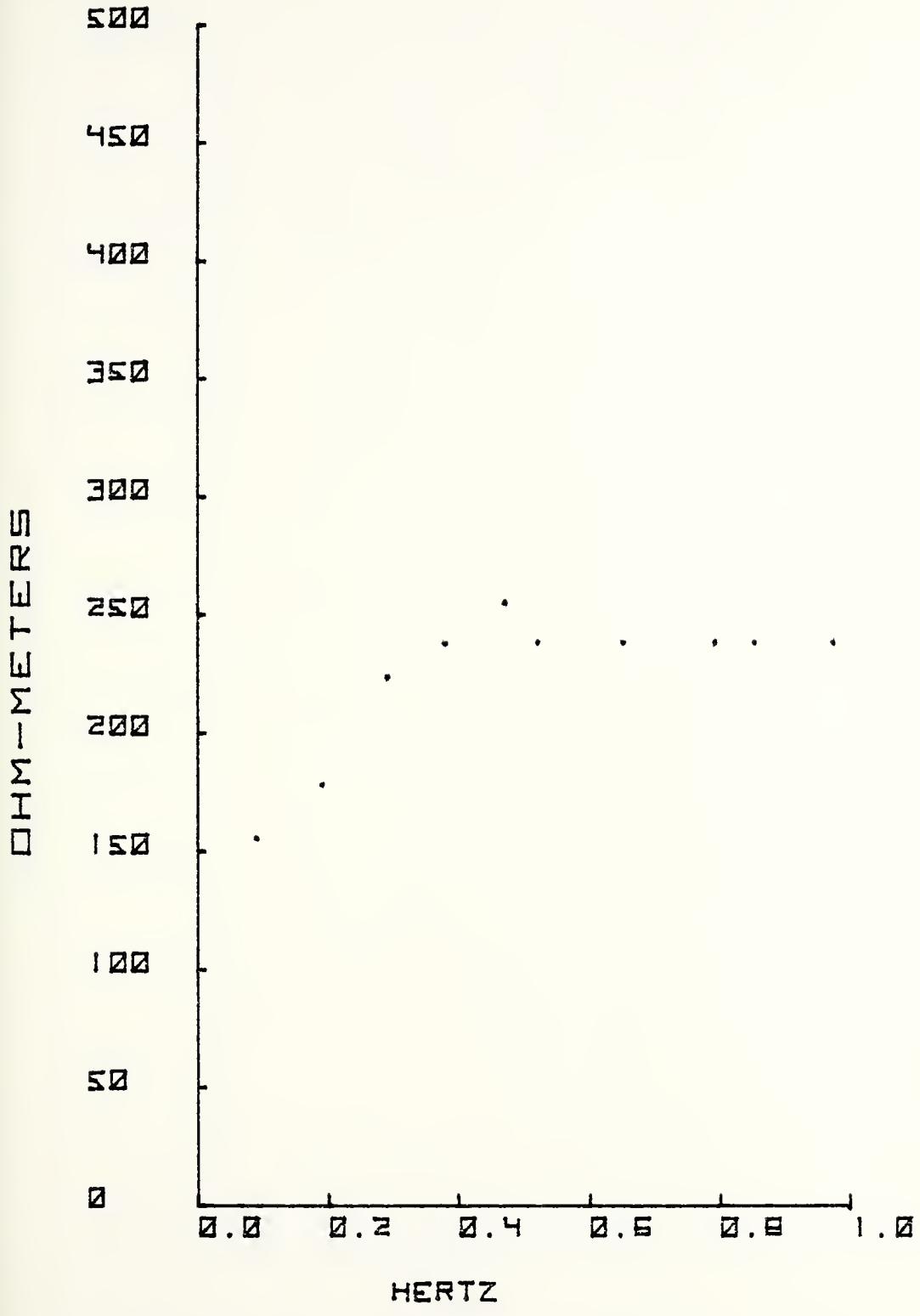

Fig. 23. Aluminum Z vs f

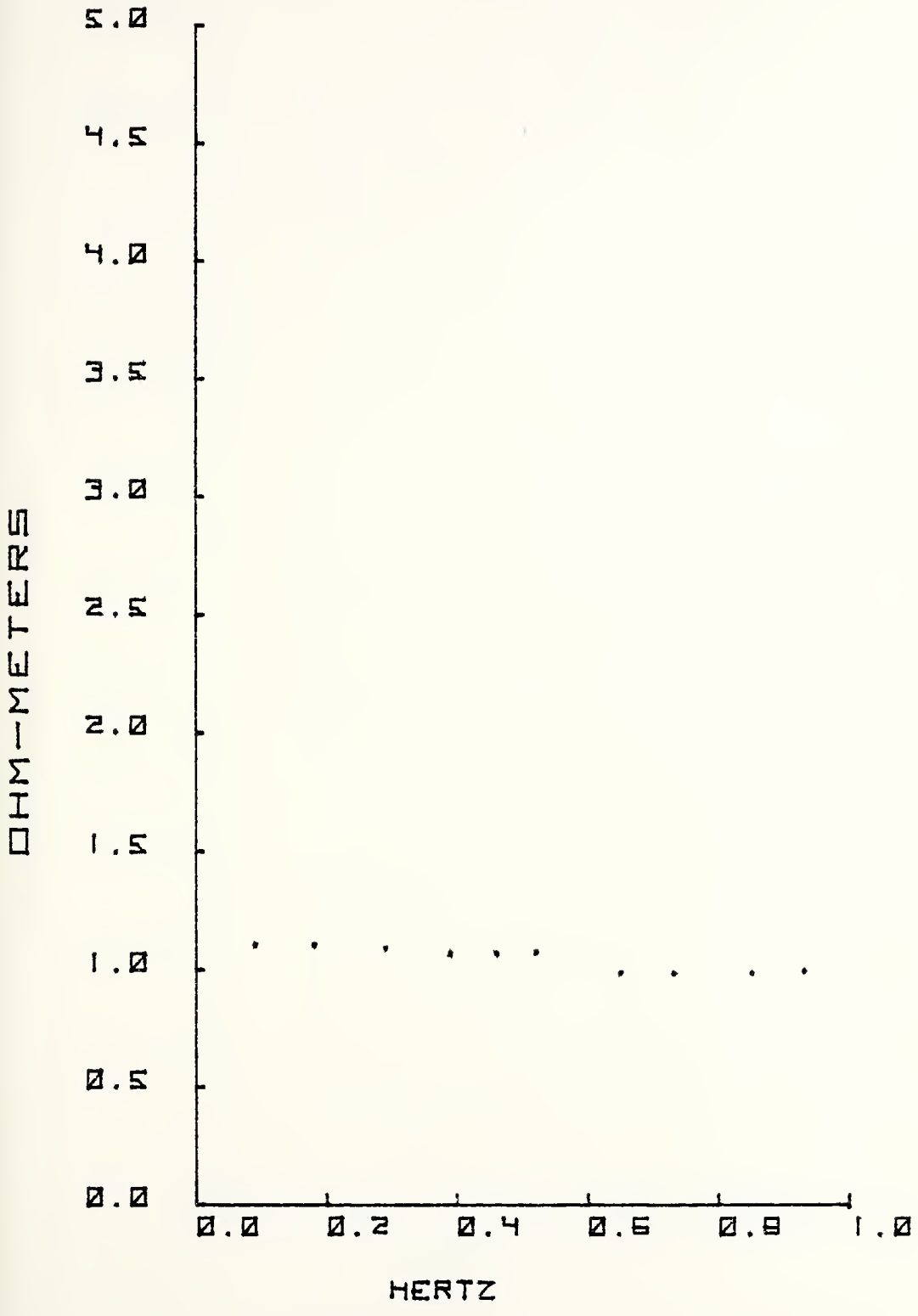

Fig. 24. Carbon Z vs f

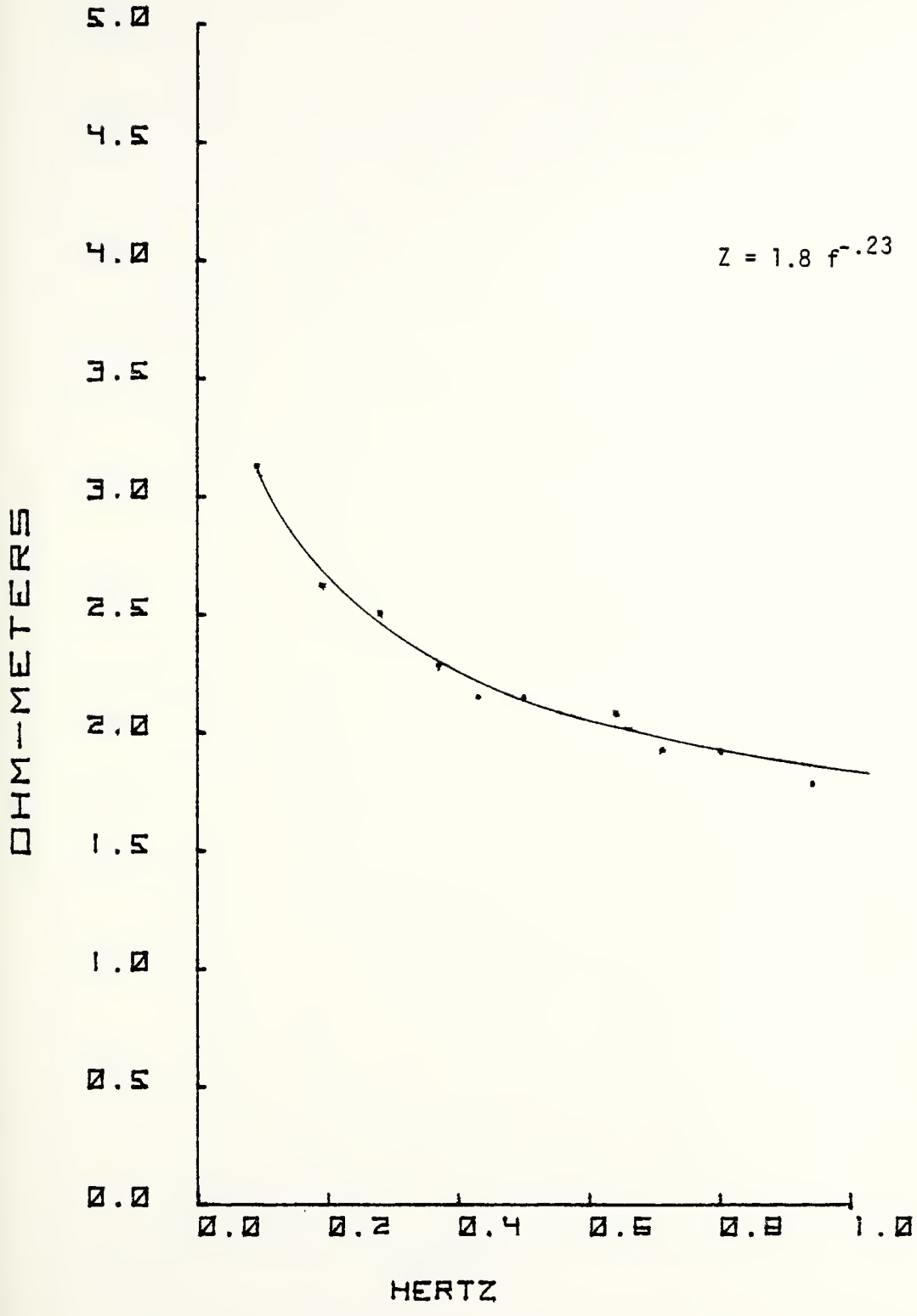

Fig. 25. Copper Z vs f

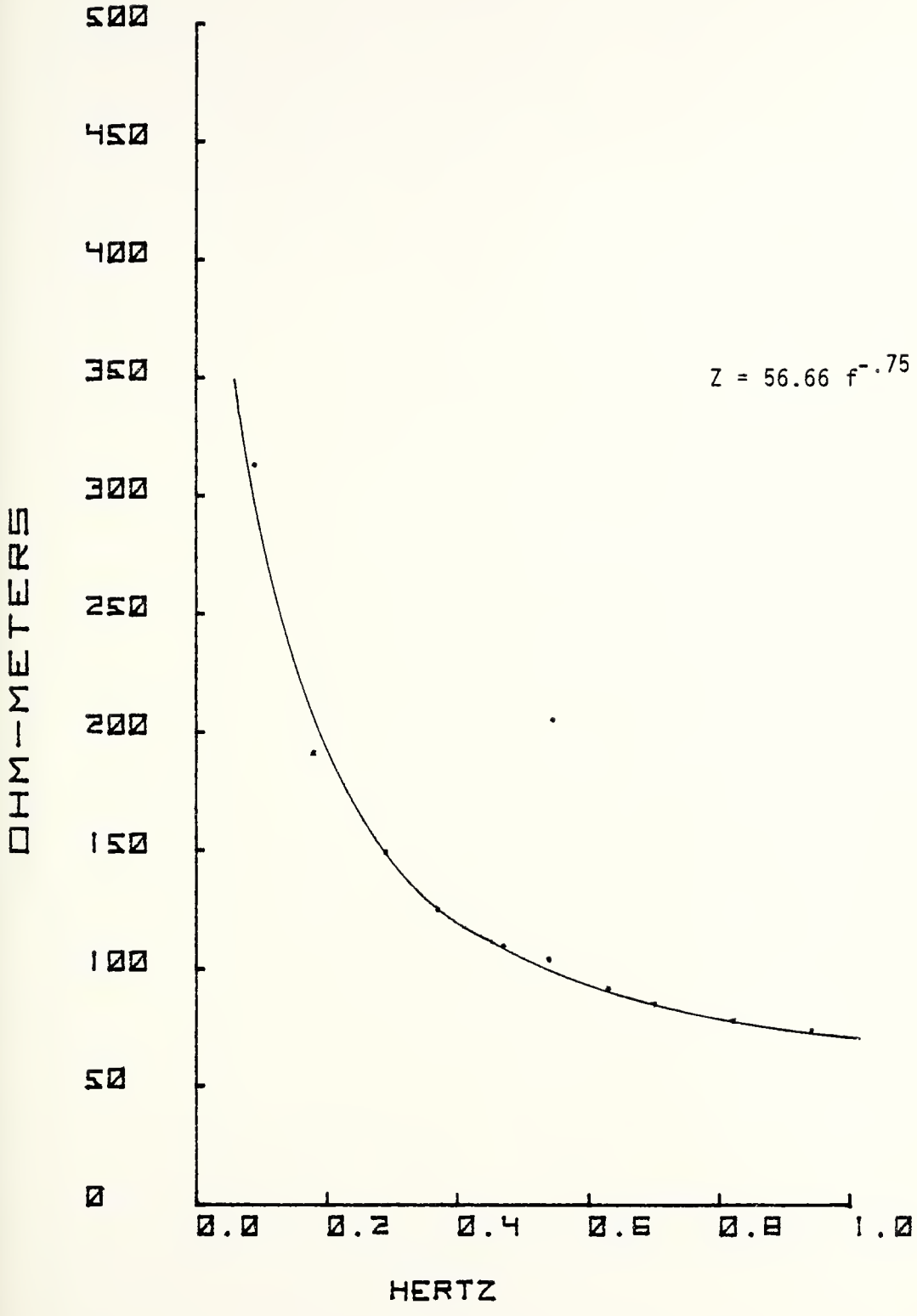

Fig. 26. Nickel Z vs f

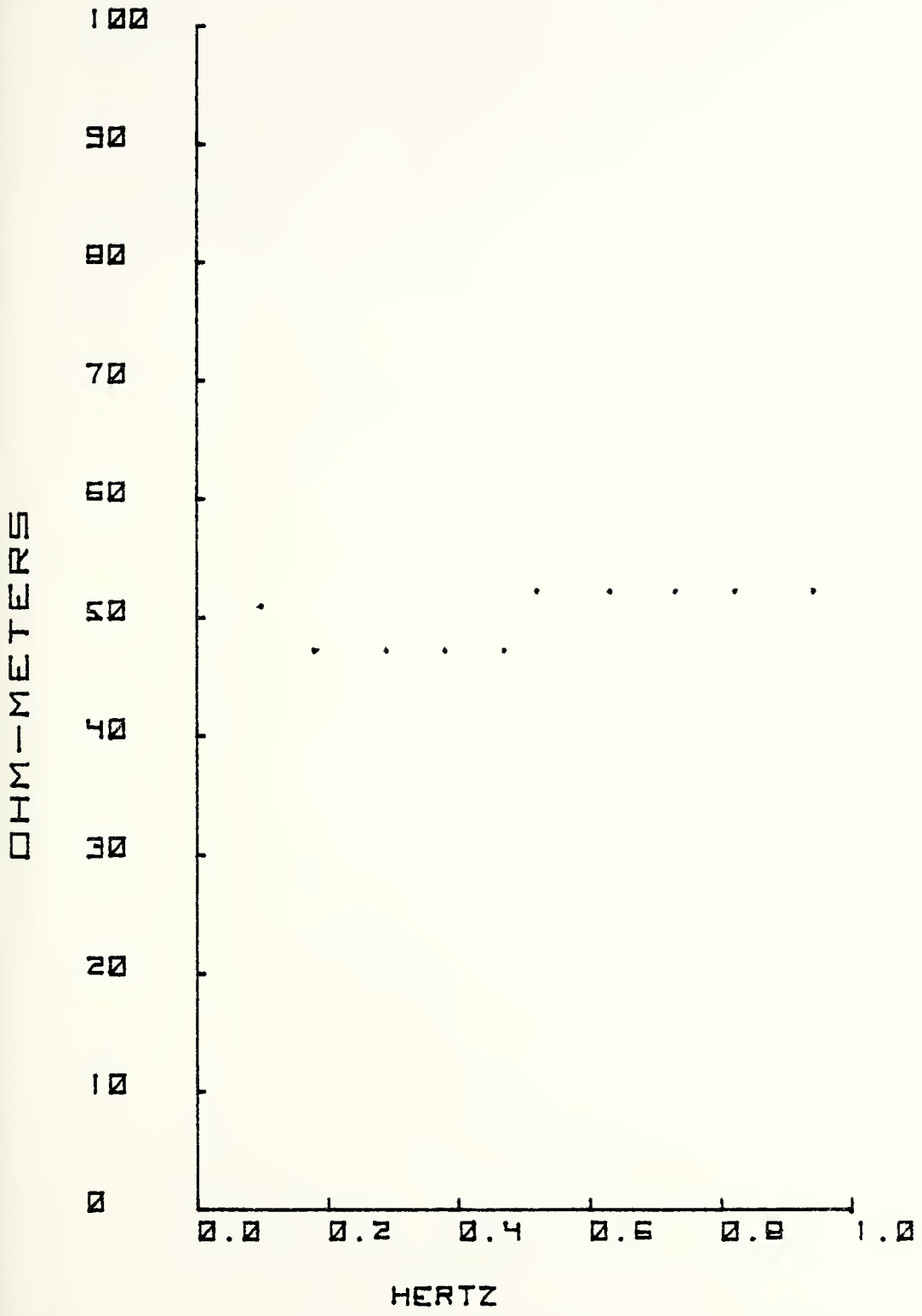

Fig. 27. Lead Z vs f

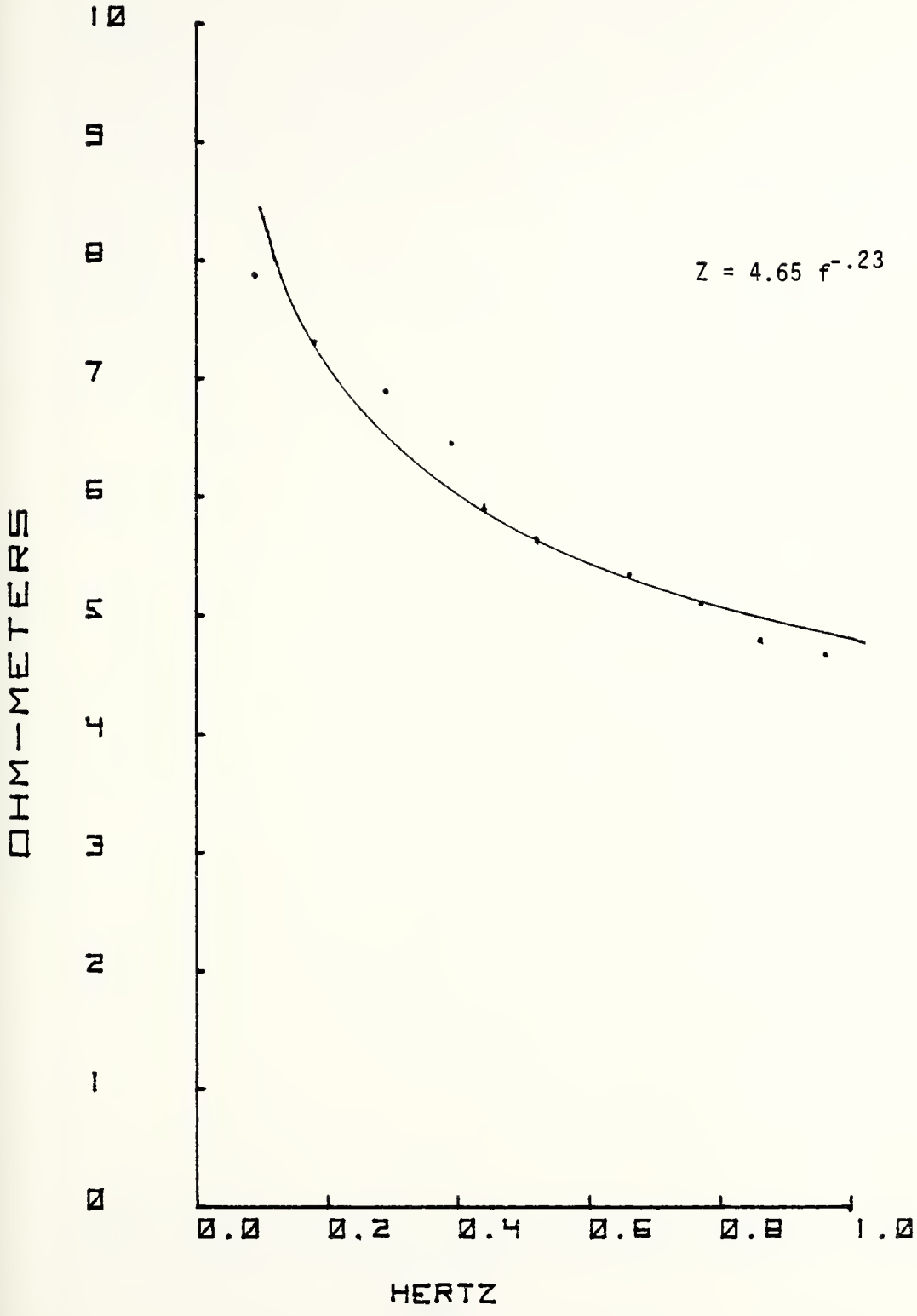

Fig. 28. Platinum Z vs f

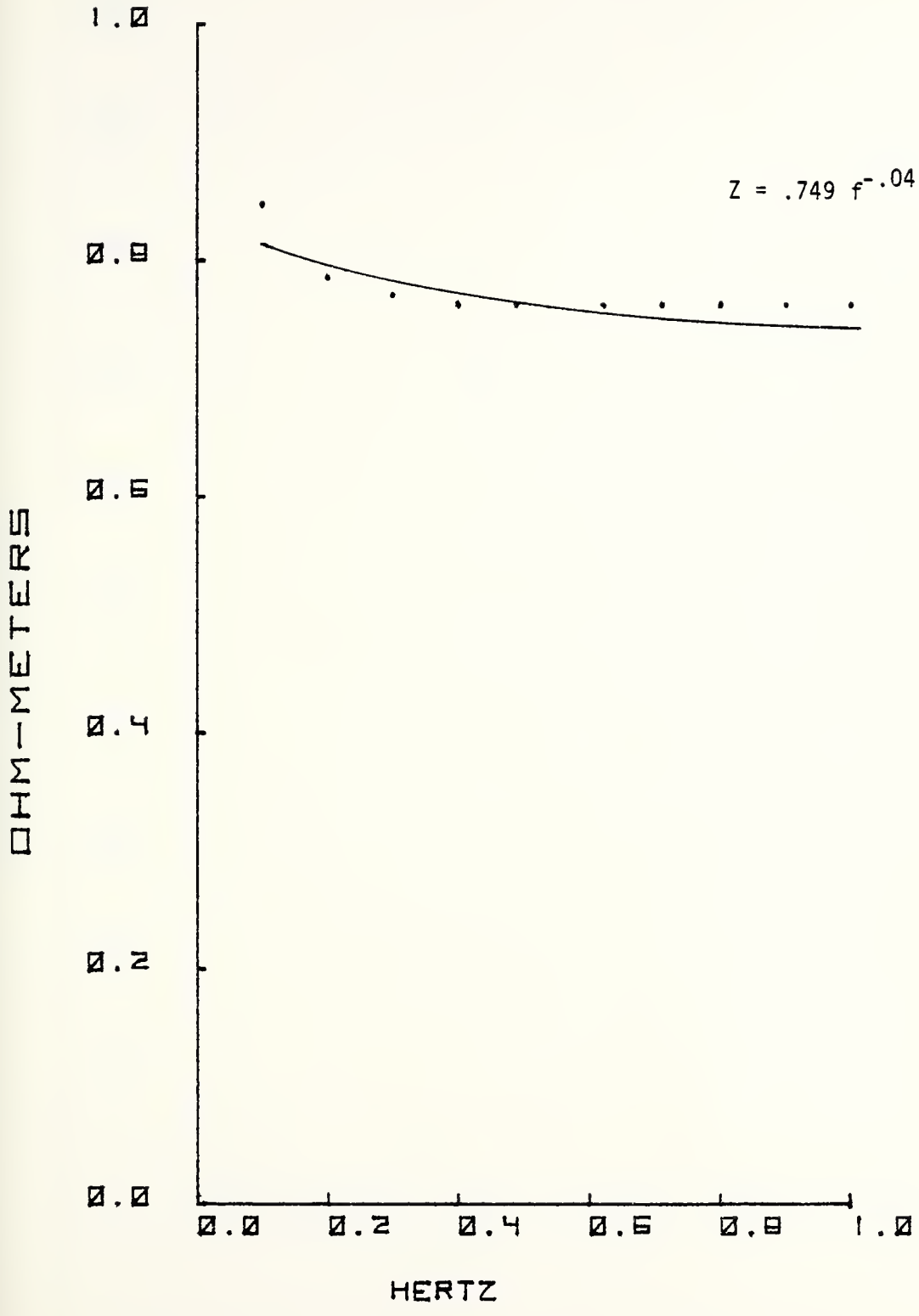

Fig. 29. Platinum Platinum-Black Z vs f

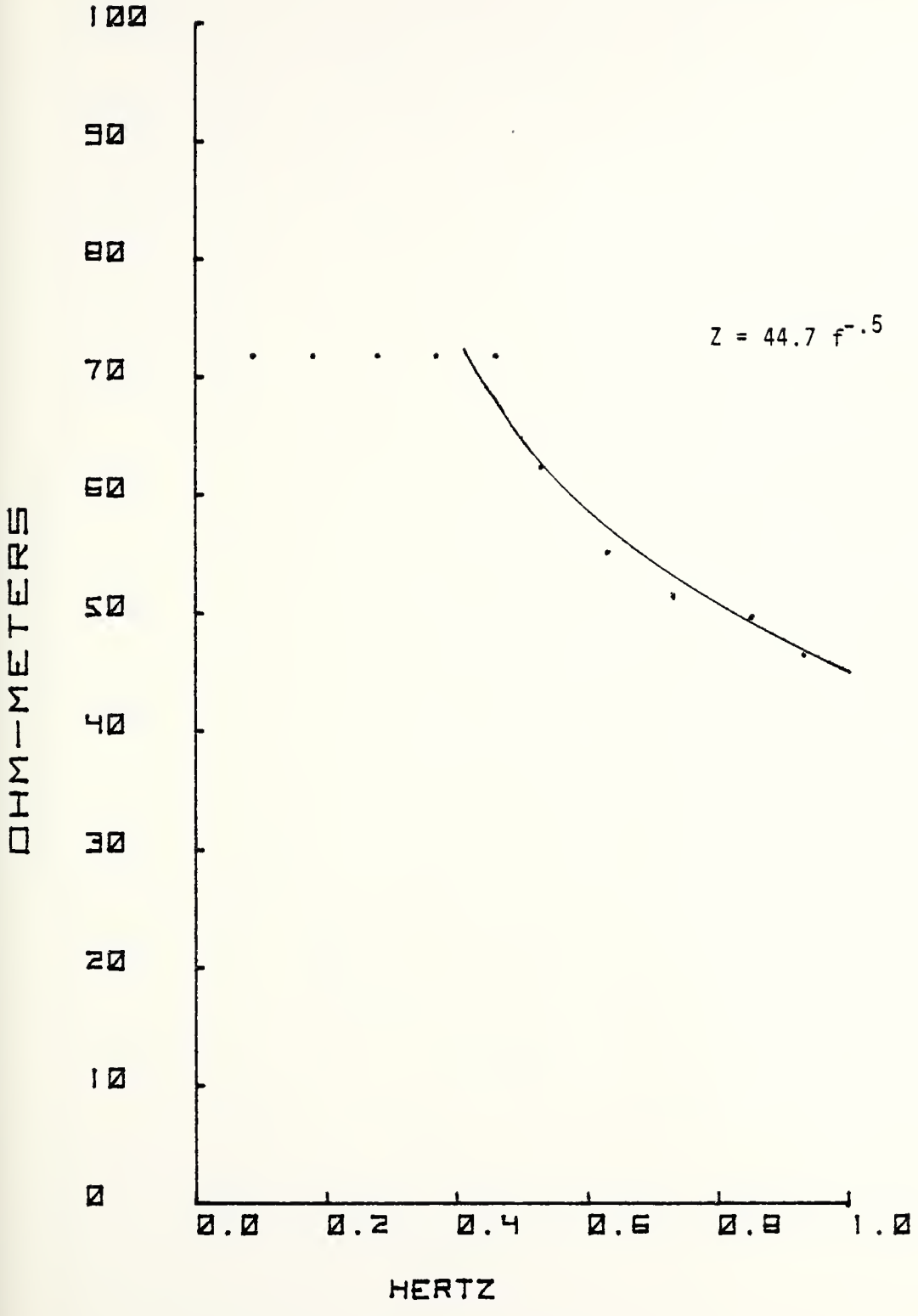

Fig. 30. Tin Z vs f

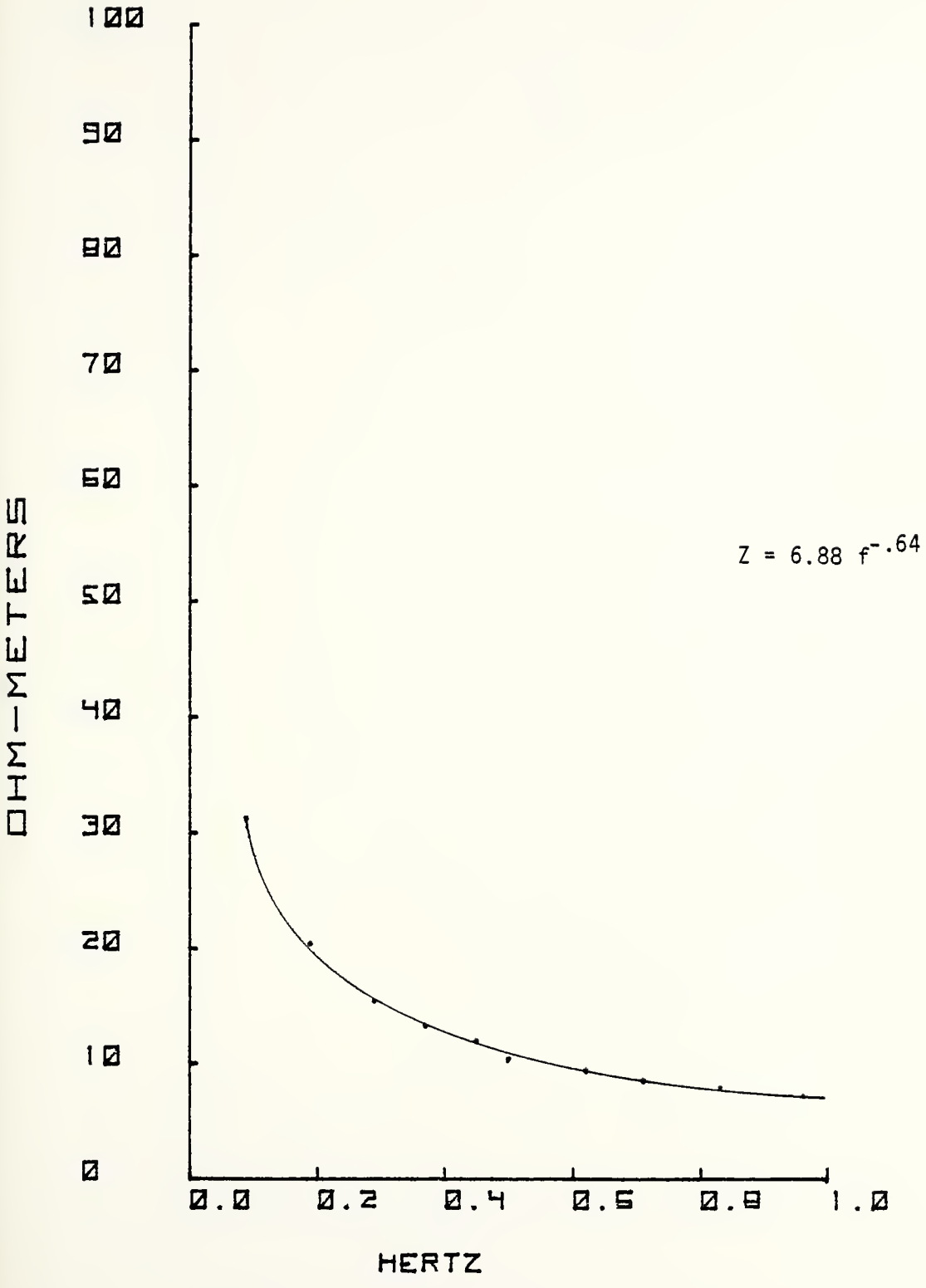

Fig. 31. Stainless Steel Z vs f

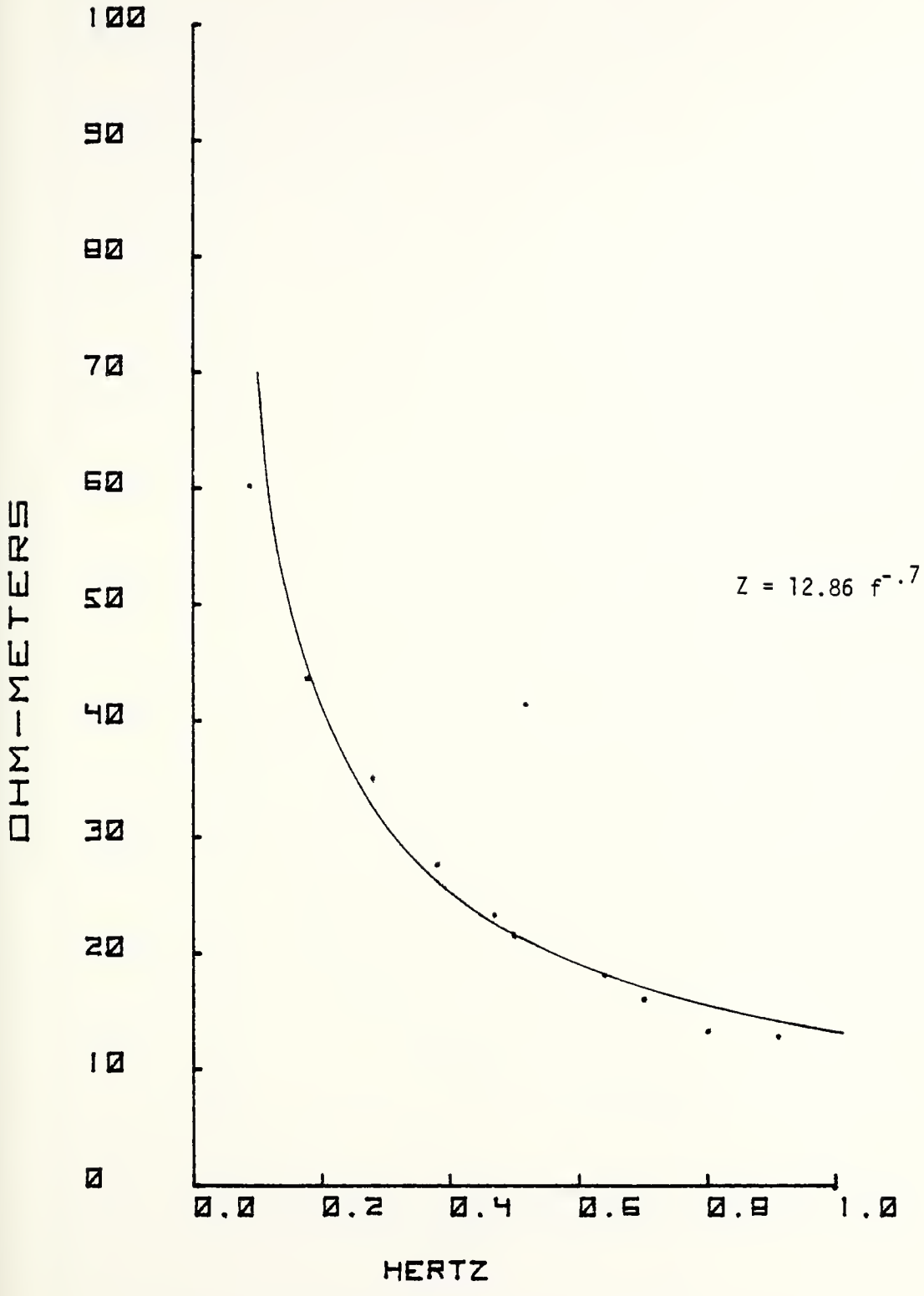

Fig. 32. Tungsten Z vs f

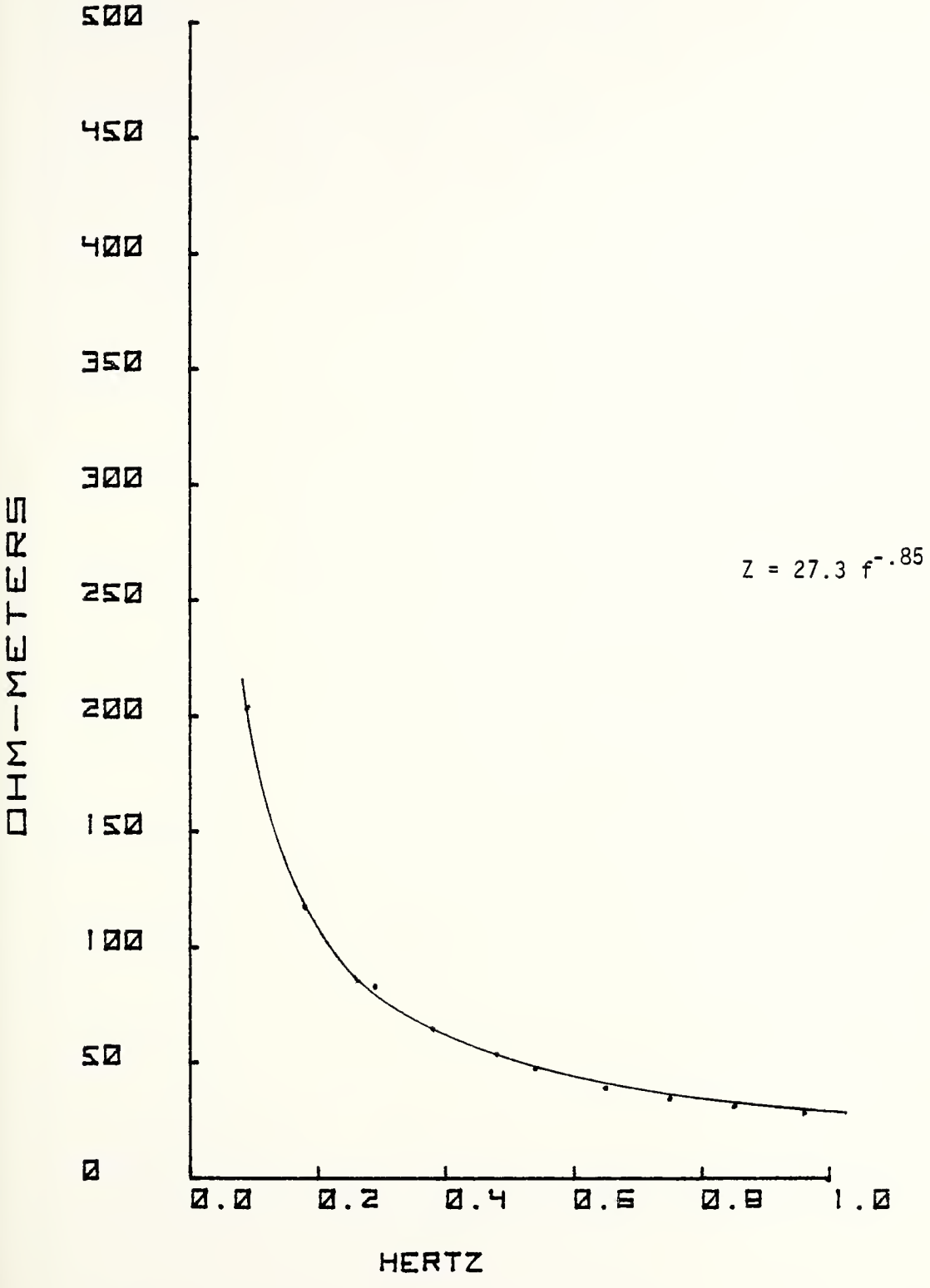

Fig. 33. Titanium Z vs f

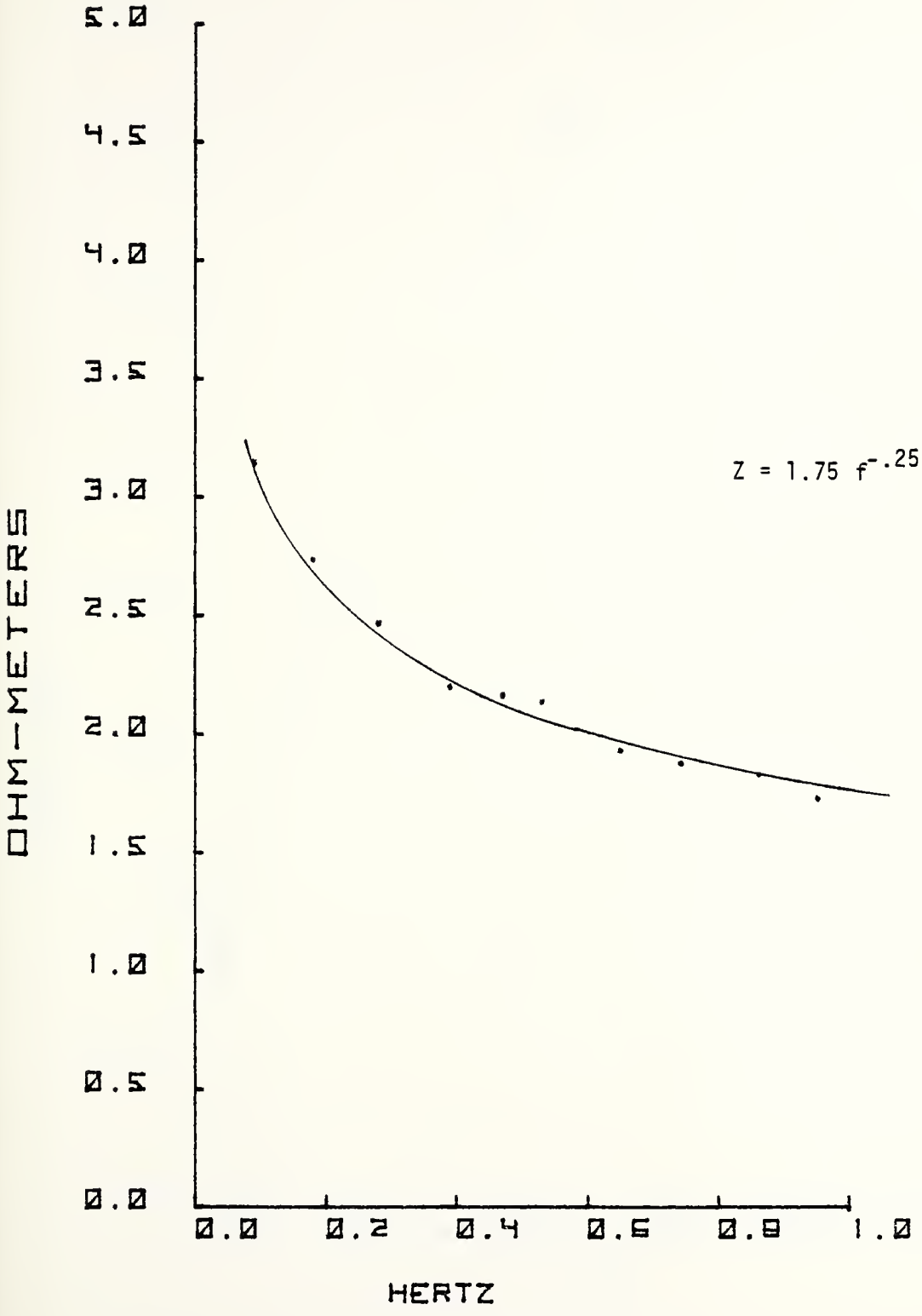

Fig. 34. Zinc Z vs f

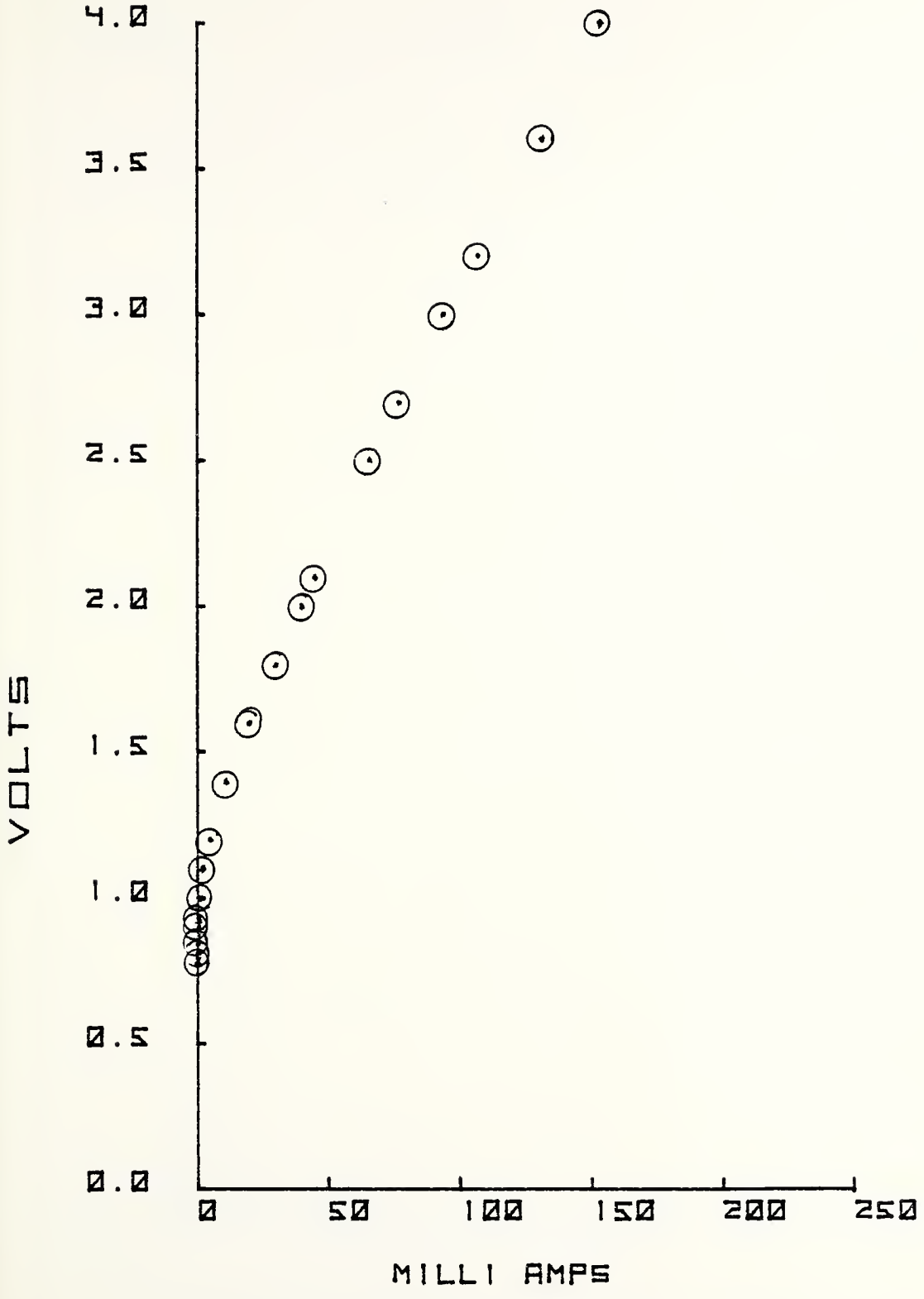

Fig. 35. Silver E vs I

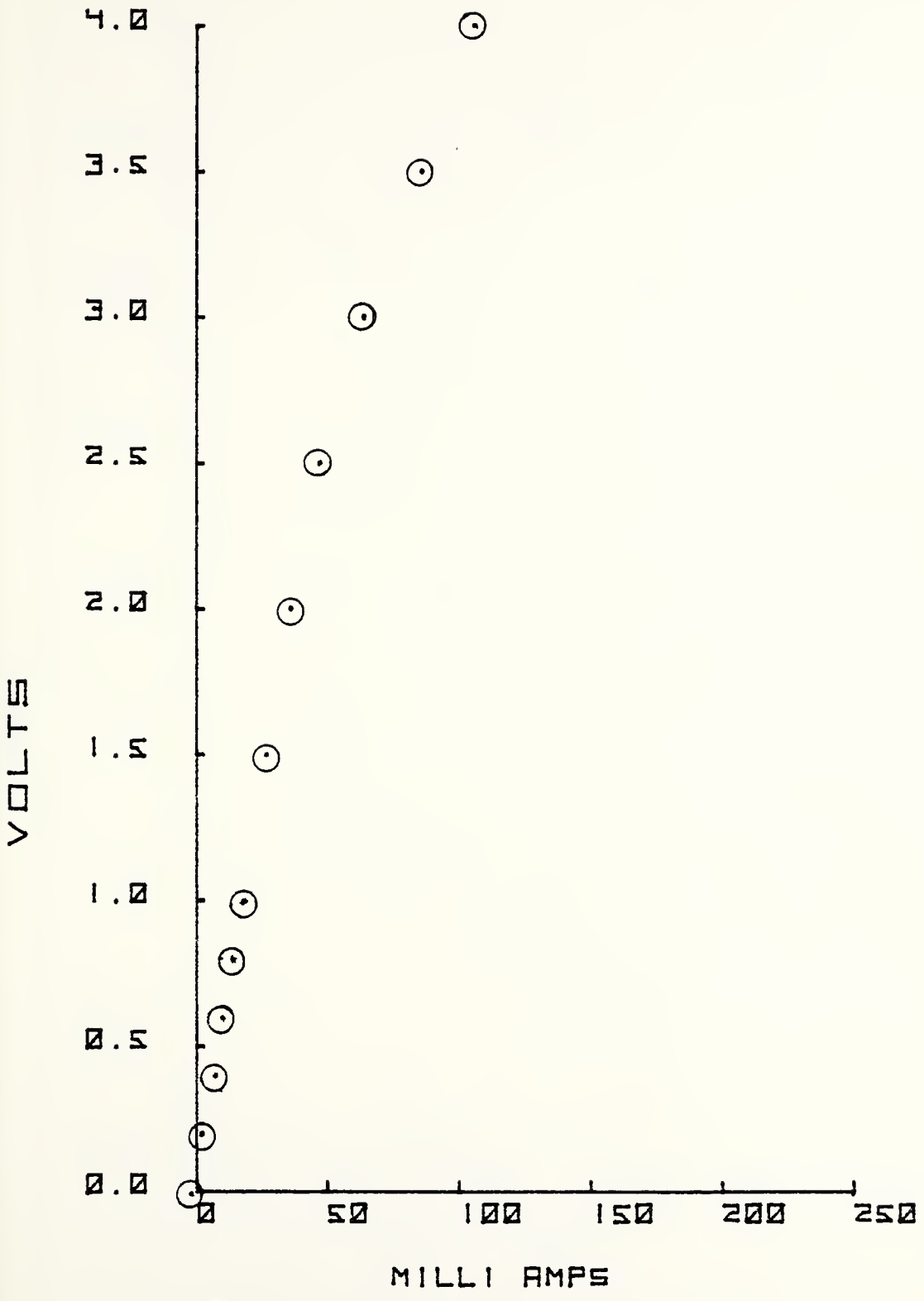

Fig. 36. Silver Silver-Chloride E vs I

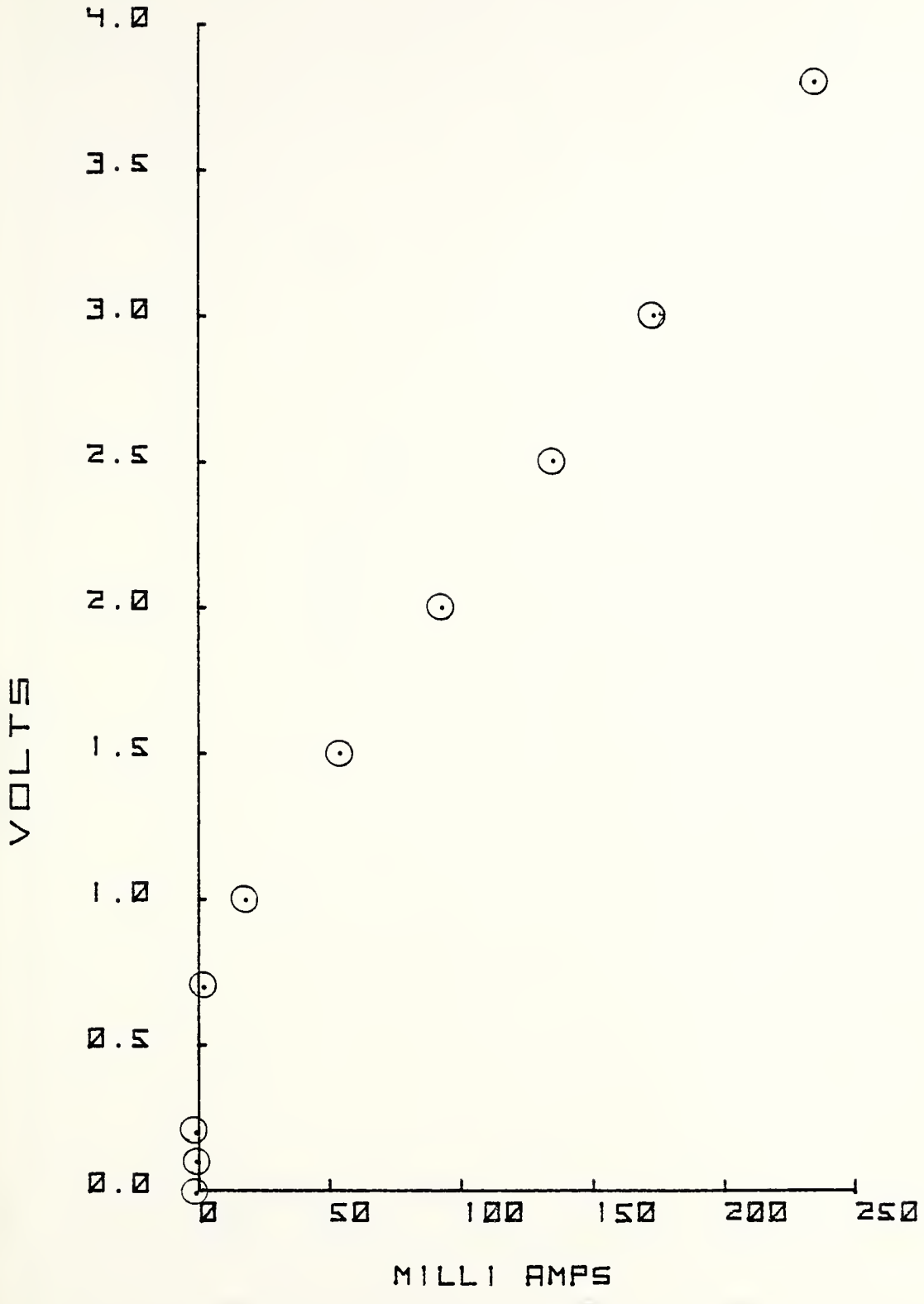

Fig. 37. Aluminum E vs I

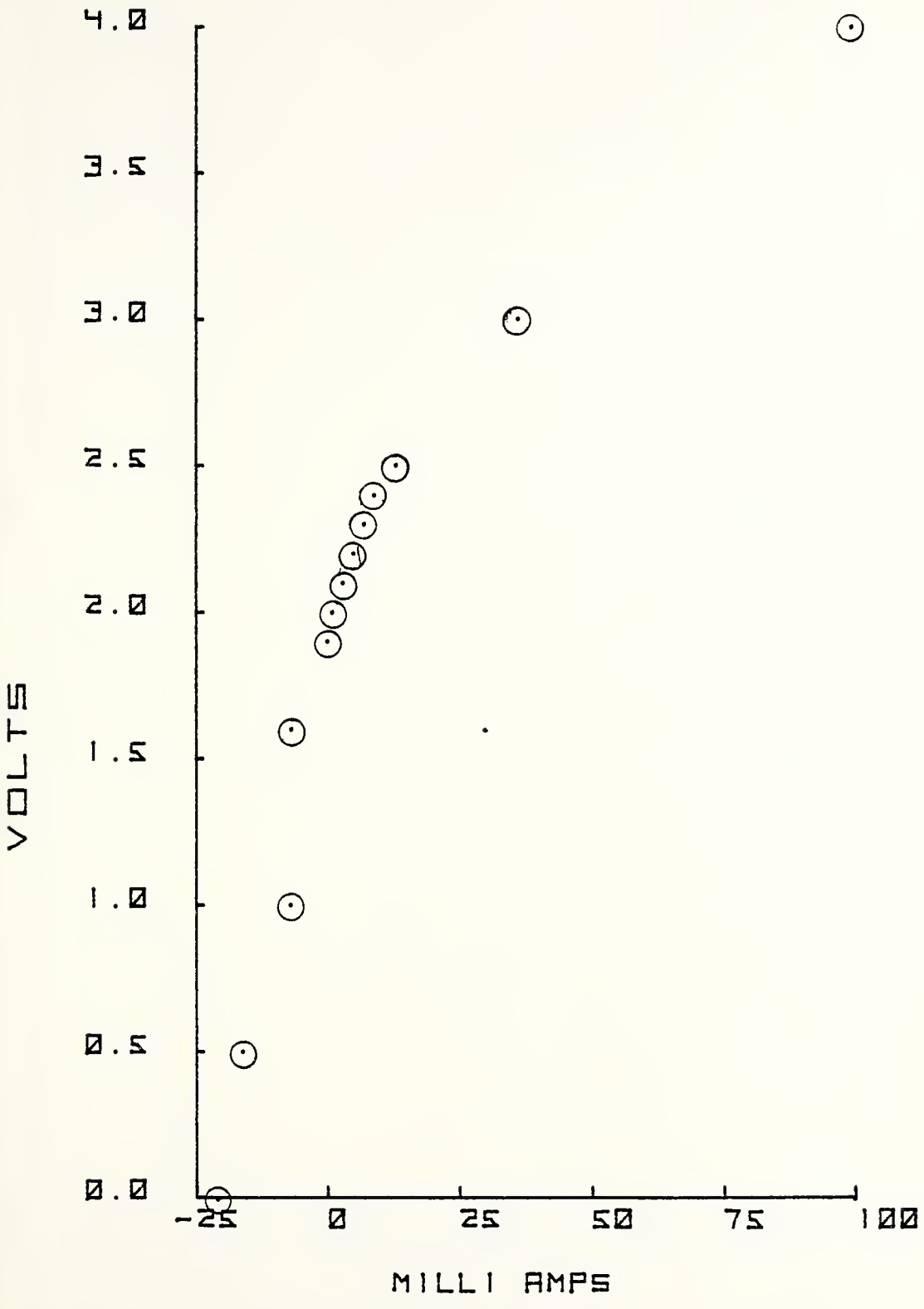

Fig. 38. Carbon E vs I

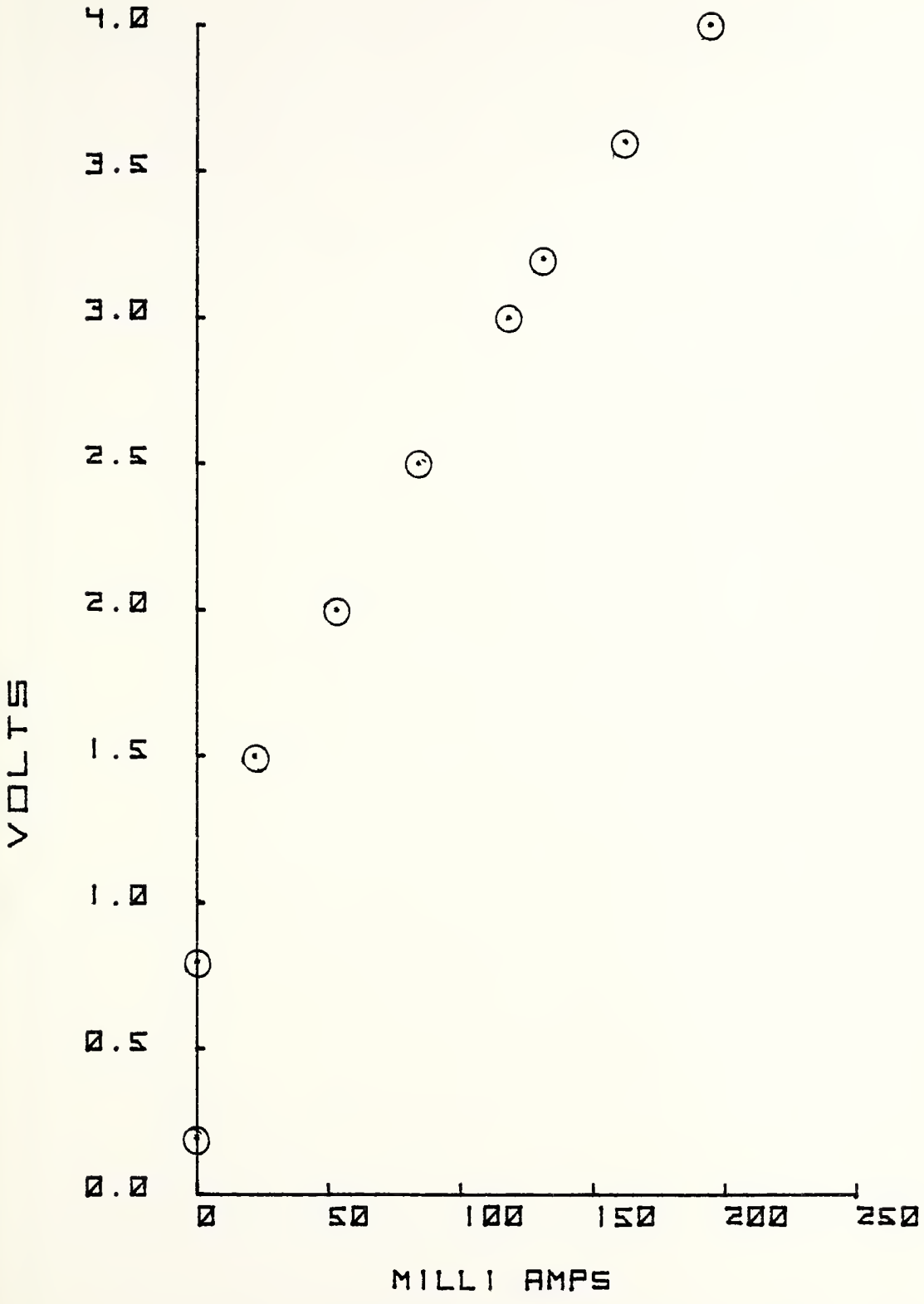

Fig. 39. Copper E vs I

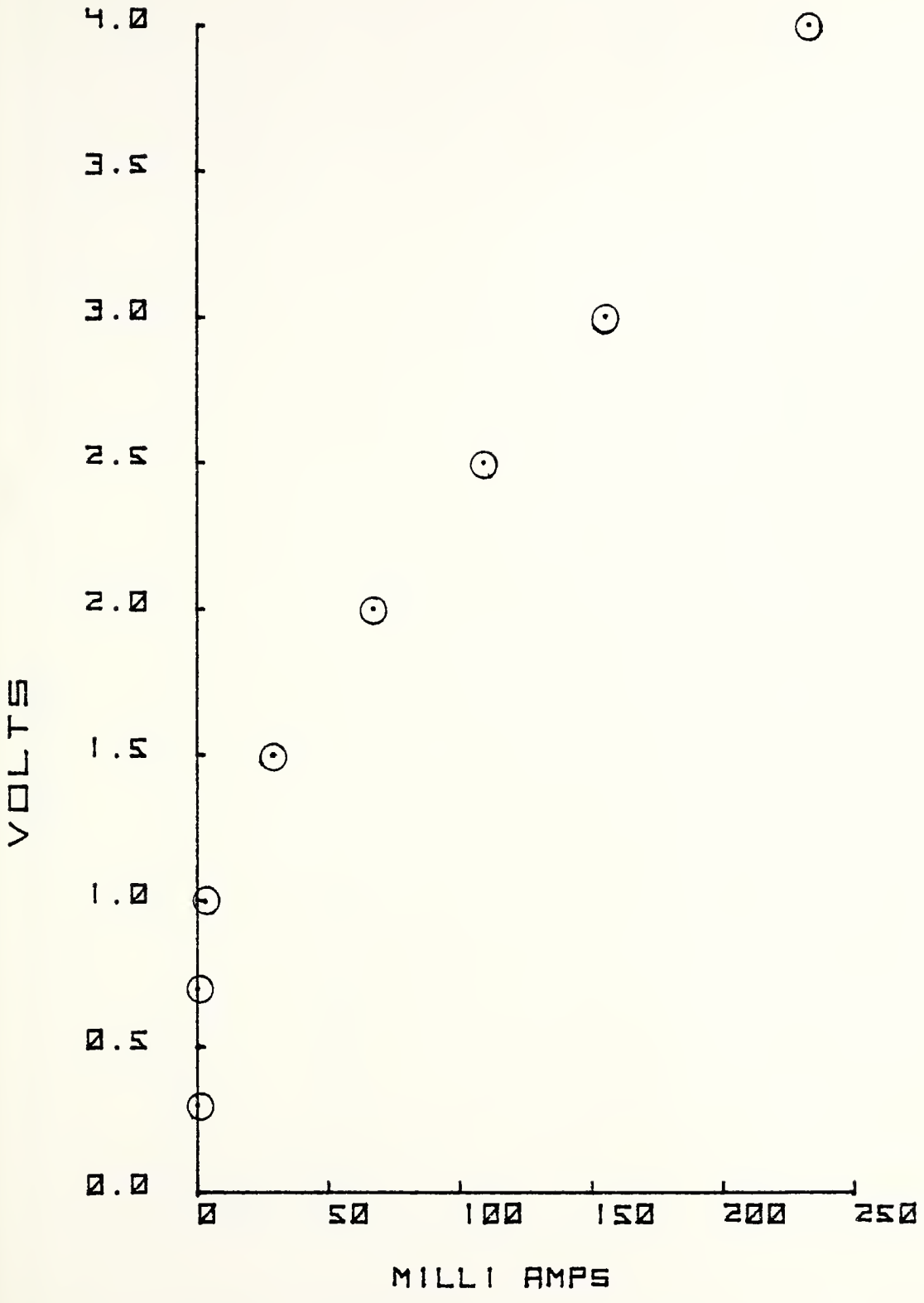

Fig. 40. Nickel E vs I

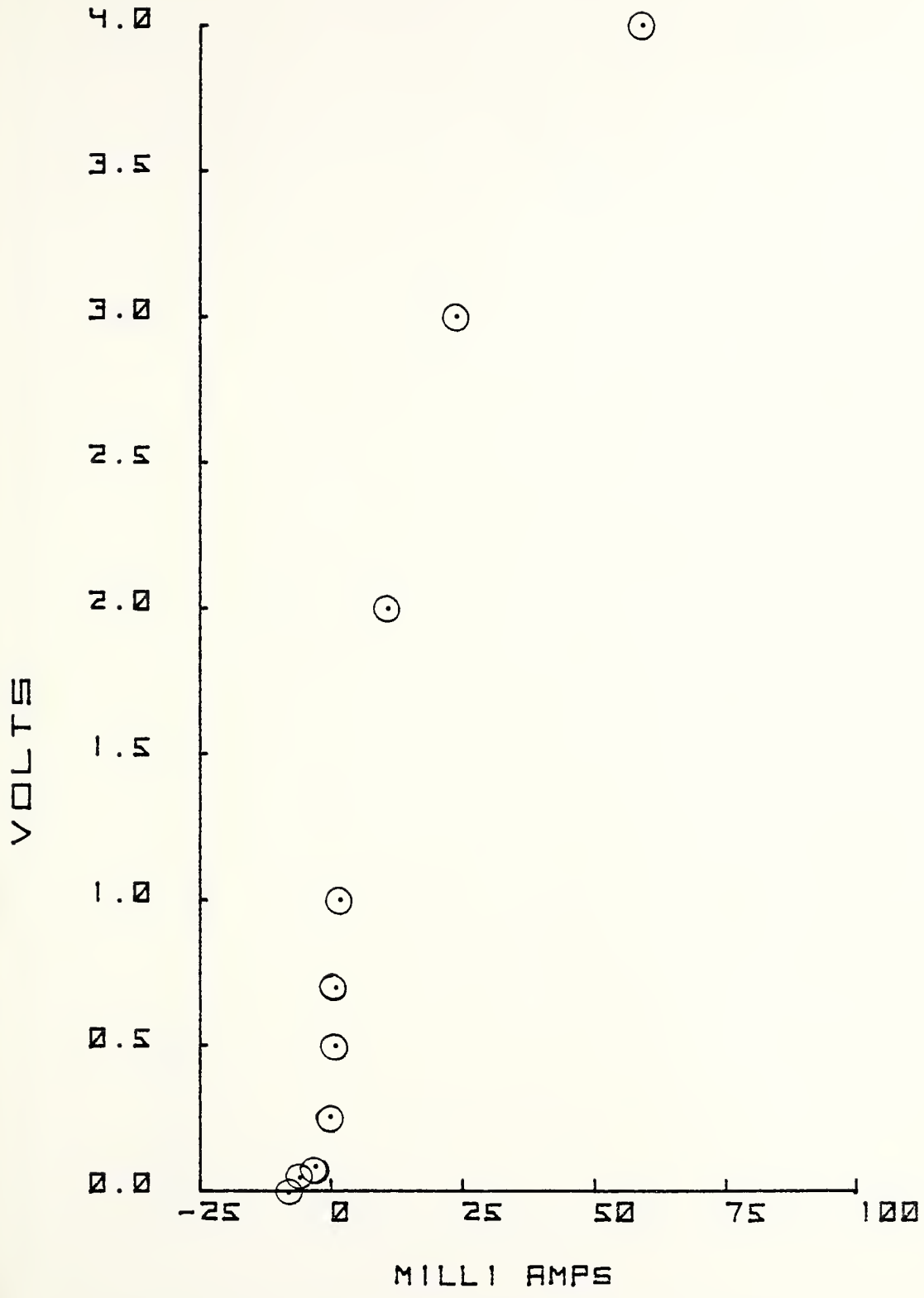

Fig. 41. Lead E vs I

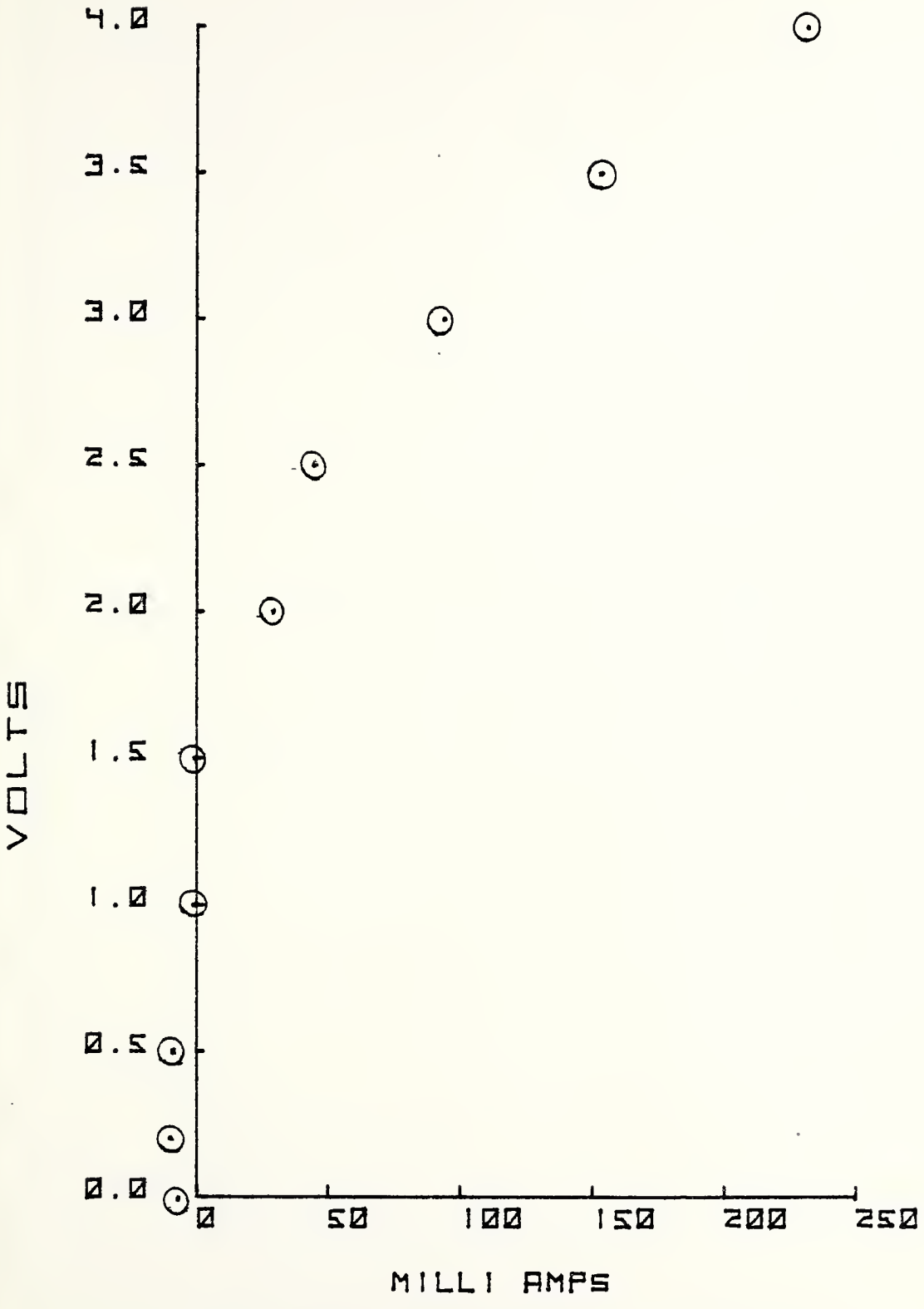

Fig. 42. Platinum Platinum-Black E vs I

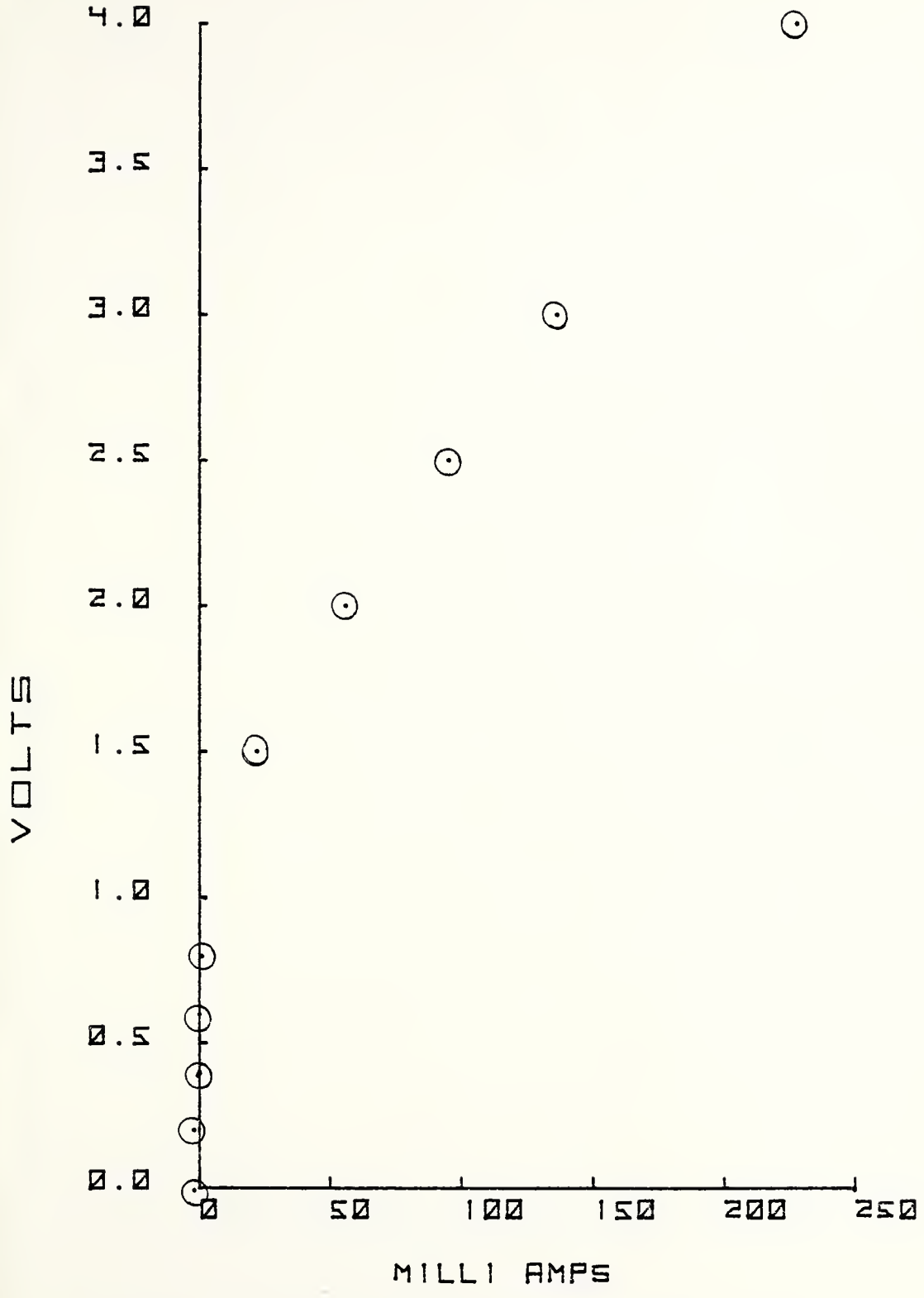

Fig. 43. Tin E vs I

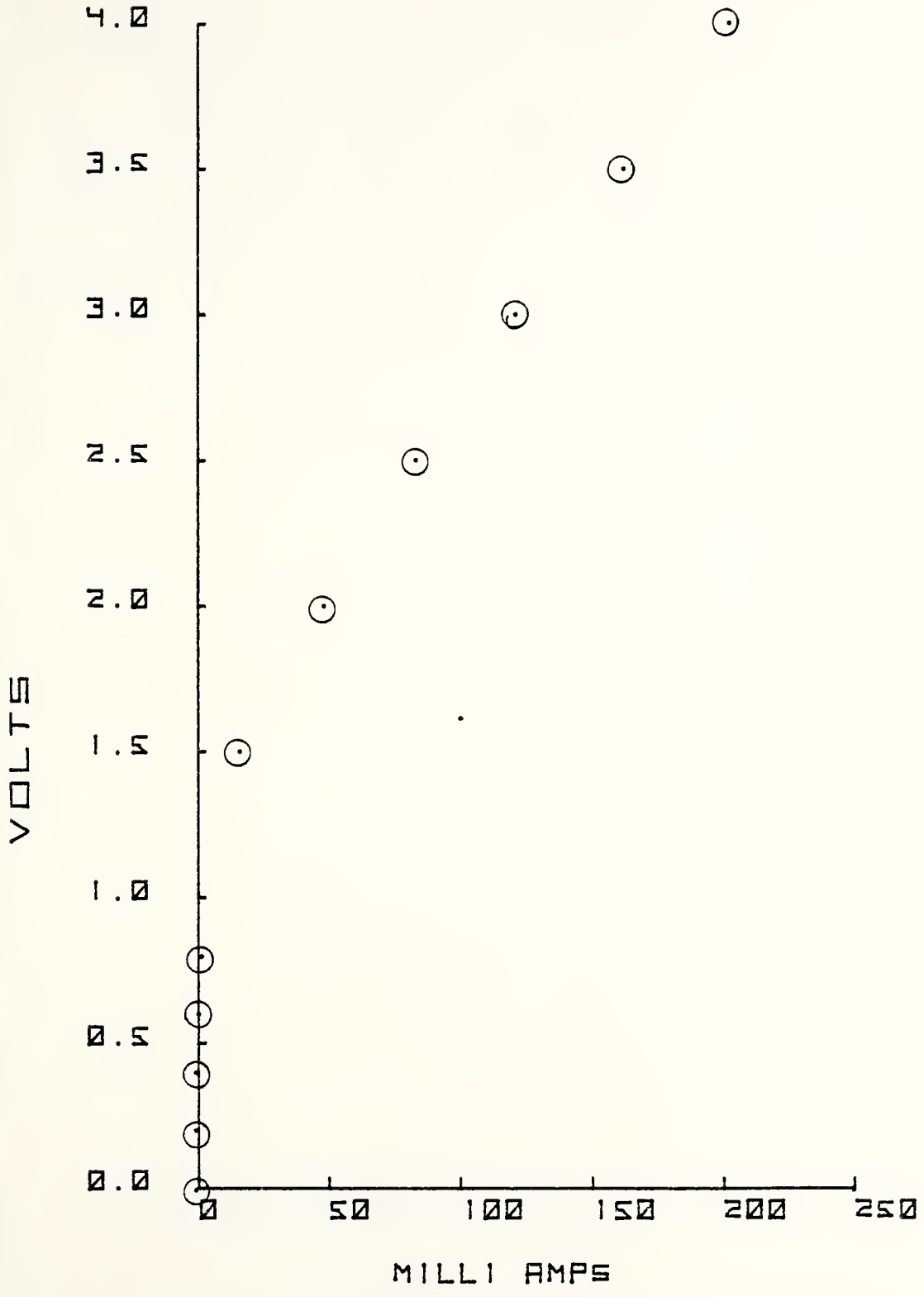

Fig. 44. Stainless Steel E vs I

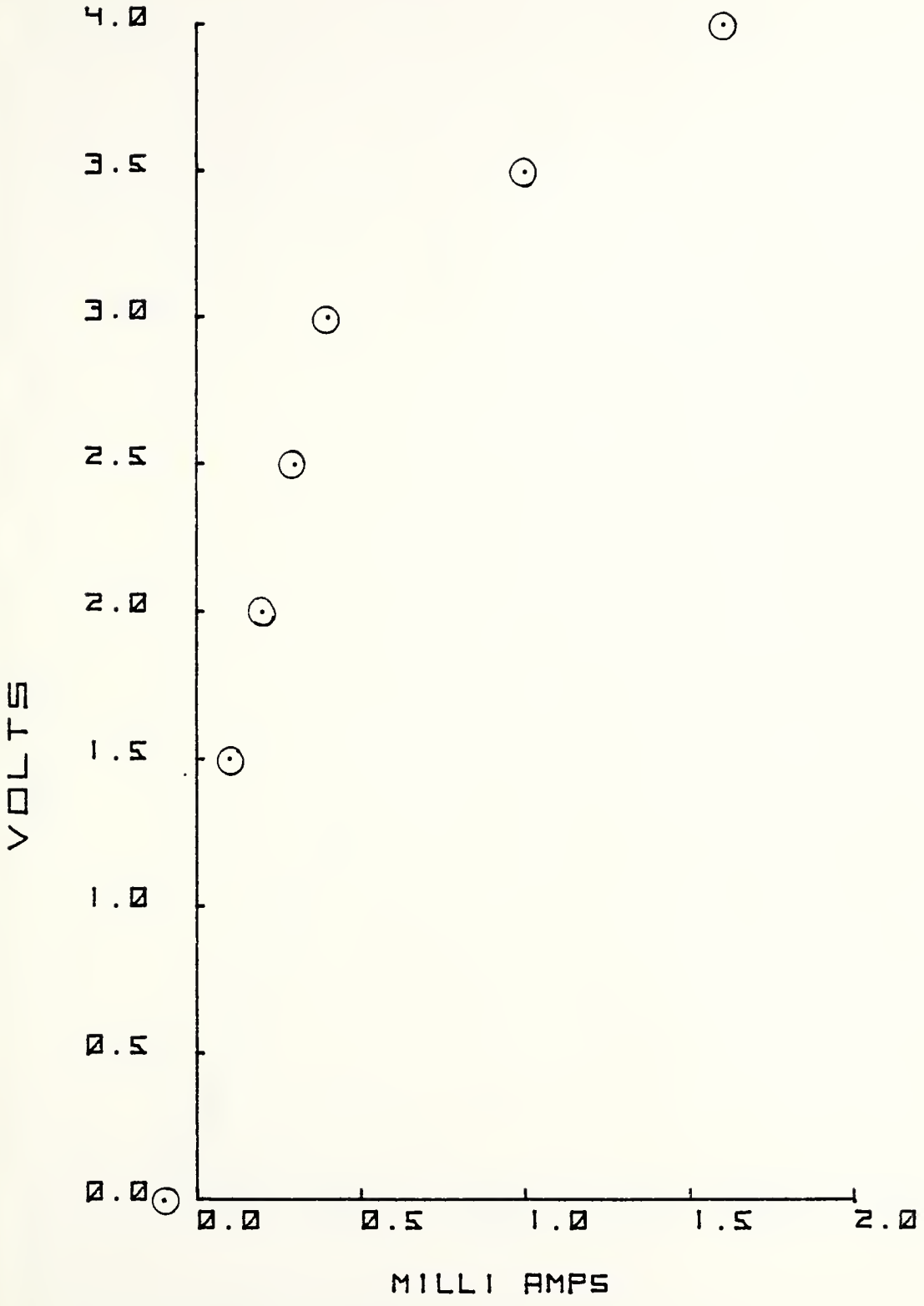

Fig. 45. Tungsten E vs I

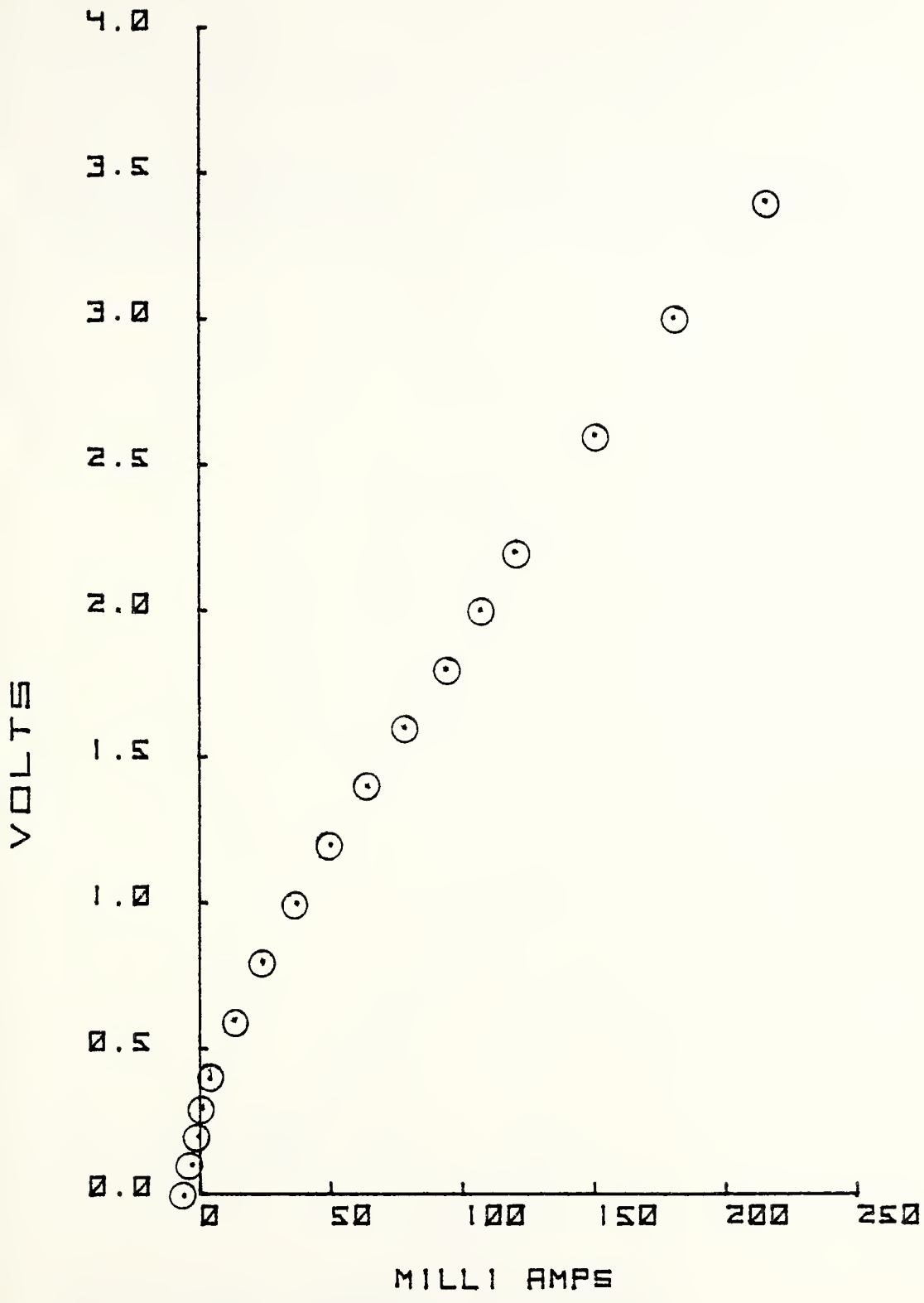

Fig. 46. Zinc E vs I

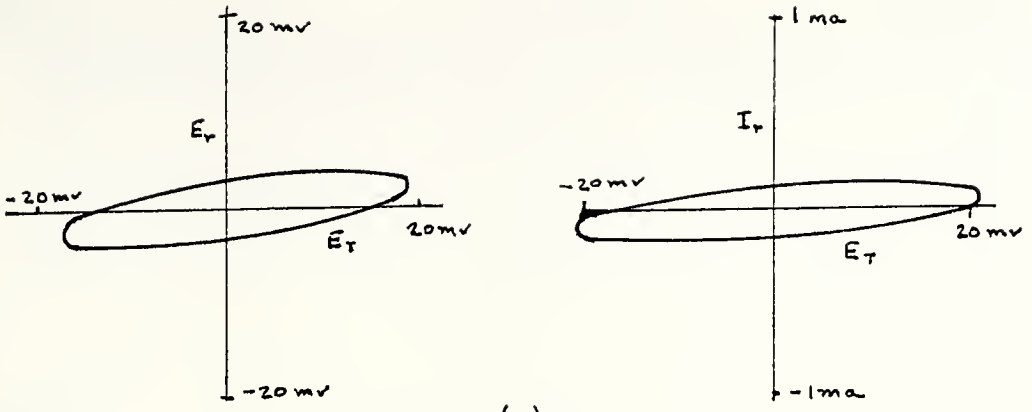

(a)

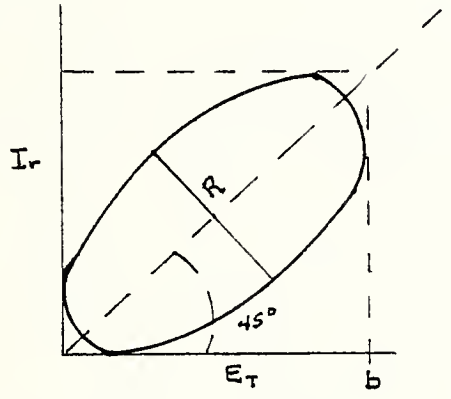

$$\phi_I = ARC\ COS\left(1 - \frac{R^2}{b^2}\right)$$

(b)

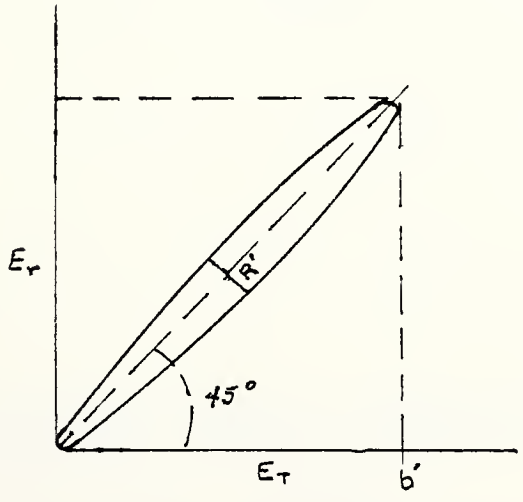

$$\phi_E = ARC\ COS\left(1 - \frac{R'^2}{b'^2}\right)$$

(c)

Fig. 47. Receiving Impedance Lissajous Patterns
(a) E_r vs E_T , I_r vs I_T
(b) I_r vs E_T phase angle
(c) E_r vs E_T phase angle

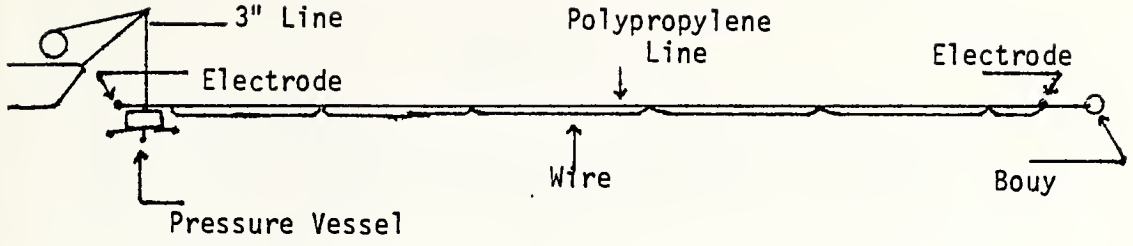

(a)

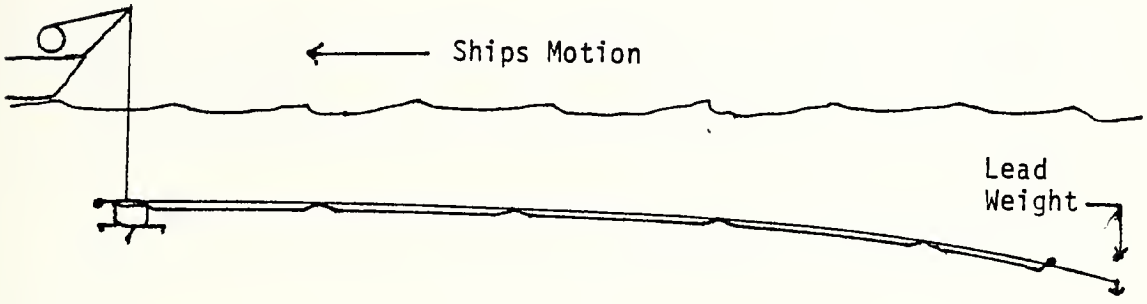

(b)

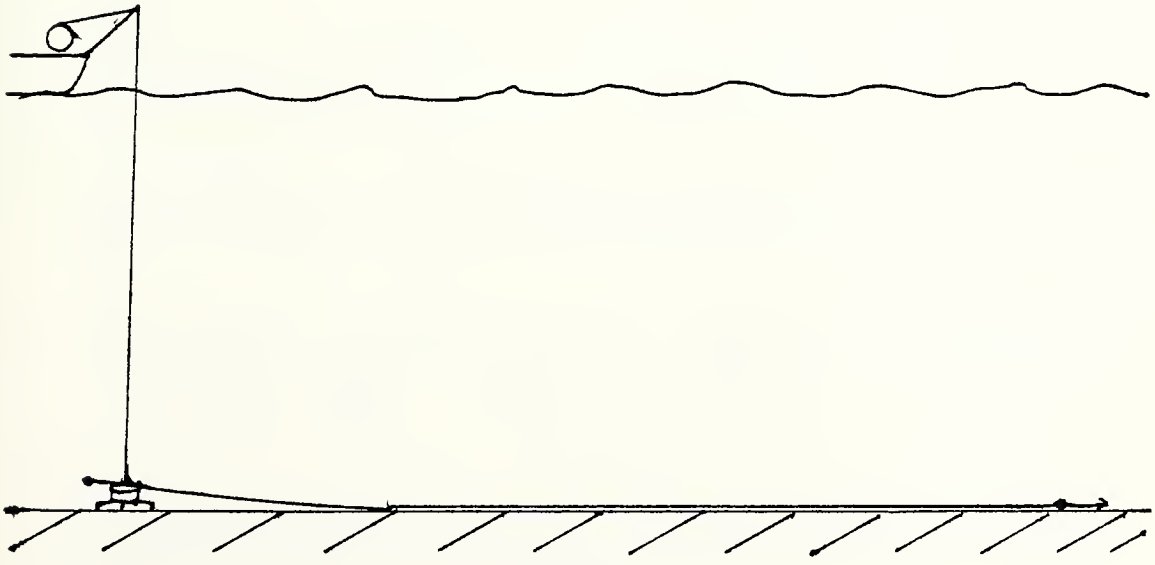

(c)

Fig. 48. Dipole Antenna Deployment
(a) On surface
(b) Lowering
(c) On Bottom

REFERENCES

1. Barry, John M., Power Spectra of Geomagnetic Fluctuations, M.S. Thesis, Naval Postgraduate School, Monterey, CA, 1978.

2. Bannister, Peter R., ELF Effective Noise Measurements Taken in Connecticut During 1976, Naval Underwater Systems Center, Newport RI, 1977. NUSC Tech Report 5681.

3. Carlson, A.B., Communication Systems, p. 118-120, McGraw-Hill, 1975.

4. Dinger, Robert J. and others, Techniques for Ocean-Bottom Measurements of Magnetic Fields with a Superconducting Magnetometer, IEEE Transactions on Geoscience Electronics, V. GE-15, No. 4, p. 228-231, 1977.

5. Dunokel and R.A. Helliwell, Whistler Mode Emissions on the OGO 1 Satellite, Journal of Geophysics Research, 74, No. 26, p. 6371, 1969.

6. Etro, J.F., Production of ULF Magnetic Noise by Ocean Surface Gravity Waves and Its Real Time Removal from Airborne Magnetometer Measurements, M.S. Thesis, Naval Postgraduate School, Monterey, CA, 1978.

7. Fenwick, R.C. and Weeks, W.L., Submerged Antenna Characteristics, IEEE Transactions on Antennas and Propagation, V. AP-11, No. 3, p. 296-305, May 1963.

8. Fraser-Smith, A.C., Bubenik, D.M. and Villard, O.C. Jr., Air/Undersea Communication at Ultra-Low-Frequencies Using Airborne Loop Antennas, Stanford Electronics Laboratories, Stanford Tech. Report No. 4207-6, 1977.

9. Fraser-Smith, A.C. and Buxton, J.L., Superconducting Magnetometer Measurements of Geomagnetic Activity in the 0.1 to 14 Hz Frequency Range, Journal of Geophysical Research, V. 80, No. 22, p. 3141-3147, 1975.

10. Gillespie, G.H., Dodney, W.N. and Buxton, J.L., Low-Frequency Noise Spectra of a Superconducting Magnetic Gradiometer, Journal of Applied Physics, V. 48, No. 1, p. 354-357, 1977.

11. Graham, G., An Account of Observations Made of the Variation of the Horizontal Needle at London in the Latter Part of 1722 and the beginning of 1723, Phil. Trans. Ray. Soc., London, V. A32, p. 96-107, 1724.

12. Hansen, R.C., Radiation and Reception with Buried and Submerged Antennas, IEEE Transactions on Antennas and Propagation, V. AP-11, No. 3, p. 207-215, May 1963.

13. Kraichman, Martin B., Handbook of Electromagnetic Propagation in Conducting Media, Naval Material Command, 1976.

14. Michels, W.C., Electrical Measurements and Their Applications, p. 162-163, Van Nostrand, 1957.

15. Moore, R.K., Effects of a Surrounding Conducting Medium on Antenna Analysis, IEEE Transactions on Antennas and Propagation, V. AP-11, No. 3, p. 216-225, May 1963.

16. Nannestad, L. Brock., EM Phenomena in the ELF Range: Natural Background Noise and Instrumentation for its Measurement, SACLANT ASW Research Center, LaSpezia, Tech. Report No. 37, 15 June 1965.

17. Oldenburg, O., Stromverdrangung Beim Seekabel Archiv fur Elektrotechnik, (Germany), V. 7, No. 11, November 1920.

18. Shadowitz, A., The Electromagnetic Field, p. 663-664, McGraw-Hill, 1975.

19. Skolnik, M.I., Introduction to Radar Systems, p. 260-265, McGraw-Hill, 1962.

20. Strarup, T., Equipment for Measuring the Horizontal Electric Field-Strength at Sea in the Frequency Interval of 1-32 Ops, SACLANT ASW Research Center, LaSpecia, Tech. Memo No. 96, 31 January 1966, unpublished.

21. Vacquier, Victor, Geomagnetism in Marine Biology, Elsevier Publishing Company, 1972.

22. Wait, J.R., The Magnetic Dipole Antenna Immersed in a Conducting Medium, Proceedings of the IRE, V. 17, p. 1244-1245, October 1952.

INITIAL DISTRIBUTION LIST

1.	Defense Documentation Center Cameron Station Alexandria, Virginia 22314	2
2.	Library, Code 0142 Naval Postgraduate School Monterey, California 93940	2
3.	Department Chairman, Code 61 Department of Physics and Chemistry Naval Postgraduate School Monterey, California 93940	1
4.	Professor Paul H. Moose, Code 61Me Department of Physics and Chemistry Naval Postgraduate School Monterey, California 93940	2
5.	LCDR Lawrence C. Dearth 124 Morrell Circle Monterey, California 93940	1
6.	Professor O. Heinz, Code 61Hz Department of Physics and Chemistry Naval Postgraduate School Monterey, California 93940	2

Thesis
D1883 Dearth
c.1 Investigation of electrode materials for low frequency electric antennas in sea water.
180131